BRYSON, JR., DAVID IRBY, M.S. Isotopic Labeling of Heme in Dehaloperoxidase and CYP102A2 for NMR Studies. (2007)
Directed by Dr. Gregory M. Raner. pp. 80

^{13}C NMR has been shown to be a powerful tool for probing the electronic distribution in paramagnetic hemes and hemoproteins. Methods that can measure the coordination state and electronic structure of the heme cofactor can be very useful for mechanistic strudies. The drawback with this technique is the low natural abundance of ^{13}C in the macrocycle, which hinders sensitivity. Advances in the use of recombinant expression systems have provided us with the resources to selectively label the heme cofactor of paramagnetic heme-containing proteins and enzymes. However, current methodologies of replacing the prosthetic heme with ^{13}C labeled heme in P450 apoproteins are not compatible with cytochromes P450 due to their denaturation upon the removal of the cofactor. We have developed a recombinant expression system, using the hemoprotein dehaloperoxidase as a model, that allows us to selectively label the heme cofactor biosynthetically by supplementing aminolevulinic acid (ALA) deficient *E. coli* Hu227 cells with synthesized isotopomers of ALA. We have also generated a recombinant plasmid encoding for CYP102A2 that will be compatible with our novel expression system, and have preliminary data indicating this method should be very useful for generating cytochrome P450 samples for ^{13}C analysis.

ISOTOPIC LABELING OF HEME IN DEHALOPEROXIDASE AND CYP102A2 FOR NMR STUDIES

by

David Irby Bryson, Jr.

A Thesis Submitted to
the Faculty of The Graduate School at
The University of North Carolina at Greensboro
in Partial Fulfillment
of the Requirements for the Degree
Master of Science

Greensboro
2007

Approved by

_____
Committee Chair

To my Mother and Father,
Without your love and support this wouldn't have been possible,
and to Stephanie,
Thank you for your love and affection.

APPROVAL PAGE

This thesis has been approved by the following committee of the Faculty of The Graduate School at The University of North Carolina at Greensboro.

Committee Chair _____

Committee Members _____

_____

_____
Date of Acceptance by Committee

_____
Date of Final Oral Examination

ACKNOWLEDGEMENTS

I would first like to acknowledge Dr. Greg Raner for his guidance and financial support through my graduate work at UNCG. I would also like to acknowledge Dr. Alice Haddy for her guidance through my undergraduate work, and for the opportunity to hold a position in her research laboratory. Finally, I would like to acknowledge Dr. Jason Reddick for his assistance through my graduate work.

TABLE OF CONTENTS

Page

LIST OF TABLES

Page

LIST OF FIGURES

Page

CHAPTER I

INTRODUCTION

I.A. Cytochrome P450

Cytochrome P450 enzymes are a family of heme-containing metalloproteins, which are capable of catalyzing a broad spectrum of oxidation reactions in both prokaryotes and eukaryotes. This class of enzymes contains a heme iron that is coordinated to a proximal cysteine thiolate.[1] The axial cysteine ligand is responsible for the characteristic Soret band absorbance at 450 nm upon the formation of the Fe(II)-CO complex.[1,2] Biologically, these enzymes are important because of their unique electronic properties that give them the ability to catalyze the oxidation of steroids, fatty acids, and xenobiotics.[1-3]

Cytochrome P450 has the ability to activate molecular oxygen. In other words, the P450 binds to O_2, and creates a very powerful and reactive oxygen species through redistribution of the electron density. Figure I.1 displays the proposed catalytic cycle of P450. Substrate binds to the active site in the first step, displacing the distal water ligand, and the heme goes from its ferric hexa-coordinate state to the ferric penta-coordinate state. A single electron, provided by an auxiliary reductase enzyme, reduces the heme iron to the ferrous state in the second step; and molecular oxygen binds to oxidize the metal center in the third step. From here, a second electron is accepted from the reductase in the fourth step to form the ferric-peroxide complex. This complex is unstable, and is quickly protonated in a fifth step to form the hydroperoxo-ferric intermediate. Next, in

the sixth step, a ferryl-oxo porphyrin cation radical intermediate species is formed upon the delivery of a second proton and a water molecule is released. This radical intermediate is also known as Compound-I, and is intermediate 6 in the figure. This intermediate reacts with the bound substrate in the seventh step to form the product, which is then free to leave the active site to be replaced by water.[1]

Figure I.1. The P450 catalytic cycle.[1]

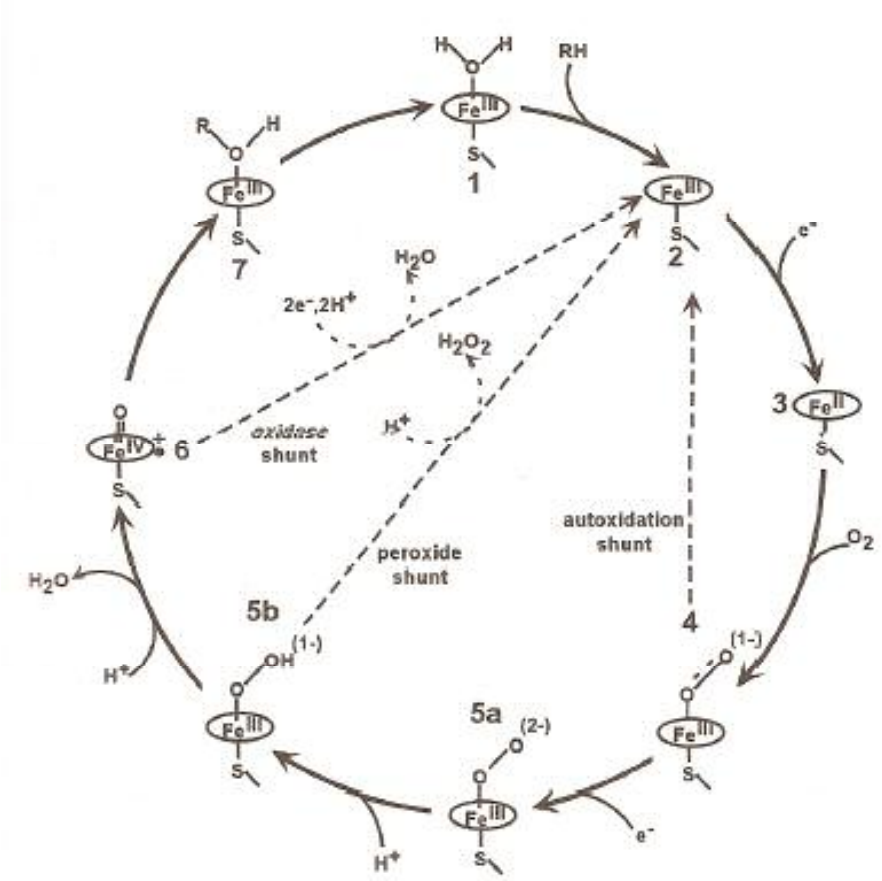

A heme, or iron-protoporphyrin IX, is the cofactor found in the active site of cytochrome P450 monooxygenase enzymes, giving these enzymes their redox capabilities.[1] It can be seen from Figure I.1 that this heme (shown as Fe^{III}) is where the

chemistry happens within the active site of this class of enzymes, thus giving the heme a crucial role in catalysis. The structure of the heme and its numbering system can be seen in Figure I.2.[4] In this system, the common names for the functional groups are used along with a number indicating its position on the macrocycle. The four meso positions are also labeled with the Greek letters α, β, δ, and γ. The core carbons refer to the atoms that are located in the pyrrole rings, including the meso carbons. These core carbons have a separate system of numbering, where the first and second carbon away from the meso carbon are called C_α and C_β respectively. C_m denotes the meso carbons.[4-5]

Figure I.2. Numbering scheme of protoheme IX. [4]

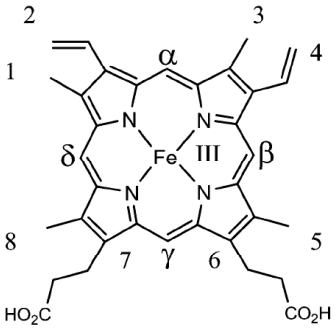

I.B. NMR spectroscopic analysis of isotopically labeled heme in hemoproteins

X-ray crystallography has emerged as the premier method for elucidating protein structure with sufficient resolution to infer mechanistic details concerning enzyme catalysis. For most proteins this method is perfectly suitable for such structure/activity studies. P450's however are somewhat elusive with regard to crystallizability. In fact, only a handful of crystal structures are currently available for this mega-family of enzymes. Furthermore, the chemistry is dictated largely by electronic delocalization

within the macrocyclic porphyrin ring system, a property that as yet cannot be probed quantitatively using crystallographic methods.

Advances in the use of recombinant expression systems, and improved spectroscopic methodologies have facilitated the use of ^{13}C-NMR in the analysis of paramagnetic heme-containing proteins and enzymes. In particular, ^{13}C-labeling of the heme cofactor provides a method of exploring the electronic structure of P450 enzymes using NMR spectroscopy. The coordination state and electronic structure of the heme cofactor is what ultimately dictates its physical and biochemical properties. Additionally, the heme iron coordination state is often indicative of the spin state. Therefore, one can use the spin state as a means for probing the ligation state of the heme iron. [4-5]

Although, it is possible to obtain information about the structural and electronic state of the prosthetic heme using ^{1}H-NMR, this type of spectroscopy has limitations when probing paramagnetic hemoproteins. One such problem arises because the delocalization of unpaired electron density is not symmetric. This ultimately causes some resonances to be resolved from the diamagnetic envelope while others are not, thus making interpretation of the spectrum more difficult. Problems also arise when heme is in the reduced form because its substituents lack isotropic shifts. These shifts are left obscured by the diamagnetic envelope and are also difficult to examine by ^{1}H-NMR.[4]

Recently, new methods have been developed using recombinant DNA technologies that allow high levels of ^{13}C and other isotopic labels to be incorporated into the prosthetic heme of hemoproteins. One study was able to demonstrate the relative ease with which the coordination state of high-spin heme proteins can be determined from ^{13}C

NMR data.[5] In this study, the ^{13}C-NMR spectra of wild-type sperm whale myoglobin (sw-Mb) and the mutant sw-Mb H64V, containing ^{13}C isotopomers of their heme, were compared in their ferric oxidation states. The wild type enzyme is hexa-coordinated in this state with the four equatorial pyrrole nitrogen ligands from the heme, and axial positions occupied by a histidine imidizole nitrogen and a water. The histidine (His-93) ligand is coordinated with the heme iron on the proximal side of the porphyrin ring, and aids in holding the heme in the active site of the protein. The water ligand is coordinated with the heme iron on the distal side of the porphyrin ring where substrates bind. A second histidine (His-64) also located on the distal side of the porphyrin ring helps to hold the water in its position.

The mutant sw-Mb is penta-coordinated in the ferric oxidation state due to the lack of the distal His-64 that would normally help to coordinate water in the axial position. The differences in the two ^{13}C-NMR spectra were the most distinct with respect to the meso carbon chemical shifts of the heme; where negative chemical shifts were observed in the wild-type sw-Mb, and positive shifts were observed in the penta-coordinated mutant sw-Mb. These chemical shifts were used as the diagnostic tool to determine the coordination state of a recently discovered monomeric periplasmic heme protein, ShuT, from *S. dysenteriae*. The coordination state for this new protein had also recently been suggested to be penta-coordinate from studies using exhaustive mutagenesis, magnetic circular dichroism, and resonance Raman techniques.[6] ^{13}C-NMR data of the ShuT enzyme that had its prosthetic heme replaced with a ^{13}C labeled heme isotopomer in the ferric oxidation state showed similar chemical shift patterns to the

mutant sw-Mb. This data was in good agreement with the mutagenesis, magnetic circular dichroism, and resonance Raman experimental data; suggesting that the coordination state of ShuT is penta-coordinate. The breakthrough, however, is that this method of determining the coordination state required only a single ^{13}C-NMR spectrum of the ShuT enzyme, compared to the multiple techniques required for the previous study with ShuT. Other newly discovered proteins have been suggested to participate in heme transport, degradation, and storage. An understanding of the electronic and coordination state properties could provide evidence for these new proteins' function.[5] Chemical shifts of the ^{13}C NMR of these proteins may allow these properties to be elucidated. Although useful for determining coordination states of hemes, a more powerful application of NMR with regard to hemoprotein analysis is the potential for probing the electronic distribution within the macrocycle.

Caignan et al. conducted studies with the hydroxide complex of *Pseudomonas aeruginosa* Heme Oxygenase containing ^{13}C labeled heme. In this study, an OH^- served as a model for the OOH^- ligand of the ferric hydroperoxide intermediate (Fe^{III}-OOH).[7] Here it was further demonstrated that the ^{13}C NMR chemical shifts were highly indicative of the heme electronic structure.

Figure I.3 demonstrates the relationship between ^{13}C chemical shifts and electronic configurations that were relevant to their study.[7] Ferrihemes with the S = 1/2, $(d_{xy})^2(d_{xz},d_{yz})^3$ electronic configuration (d_π) have their spin delocalization into the porphyrin 3e(π) orbital. It can be seen in Figure I.3 that the major electron density is centered on C_β in this configuration. That is also expressed through the corresponding

^{13}C-NMR data of Figure I.3(a), where the C_β peak is shifted the farthest downfield. The same logic follows for the C_α and meso carbons (C_m). C_α has a small amount of electron density corresponding to the small downfield shift, and C_m has a negligible amount of electron density centered on it; translating into a very small chemical shift. Ferrihemes with the S = ½, $(d_{xy})^1$ electron configuration have their spin delocalization mainly into the porphyrin $3a_{2u}(\pi)$ orbital. This configuration has the most electron density centered on the C_m carbons and a small amount of electron density centered on the other two core carbons. This is also supported through the ^{13}C-NMR data in Figure I.3(b), where the chemical shift corresponding to the C_m carbons is the furthest downfield. It can be seen that the C_α carbon has a substantial upfield shift where one might expect none, but this is due to the spin polarization from the C_m core carbons. Finally, ferrihemes with the S = 3/2 spin state show downfield shifts in the ^{13}C-NMR data that are consistent with a large amount of electron density centered on the C_α and C_β core carbons. The substantial C_m chemical shift is due to spin polarization from the nearby C_α core carbons, as the C_m orbital has no electron density.

Figure I.3. Left; Typical porphyrin core ^{13}C chemical shifts for (a) Fe^{III}-porphyrinates with the S = ½, d_π electron configuration, (b) Fe^{III}-porphyrinates with the S = ½, $(d_{xy})^1$ electron configuration, and (c) Fe^{III}-porphyrinates with the S = 3/2, $(d_{xy})^2(d_{xz},d_{yz})^2(d_{z2})^1$. Right; Schematic representation of the $3a_{2u}(\pi)$ and $3e(\pi)$ porphyrin orbitals. Relative circle sizes correspond to the calculated electron density at that position.[7]

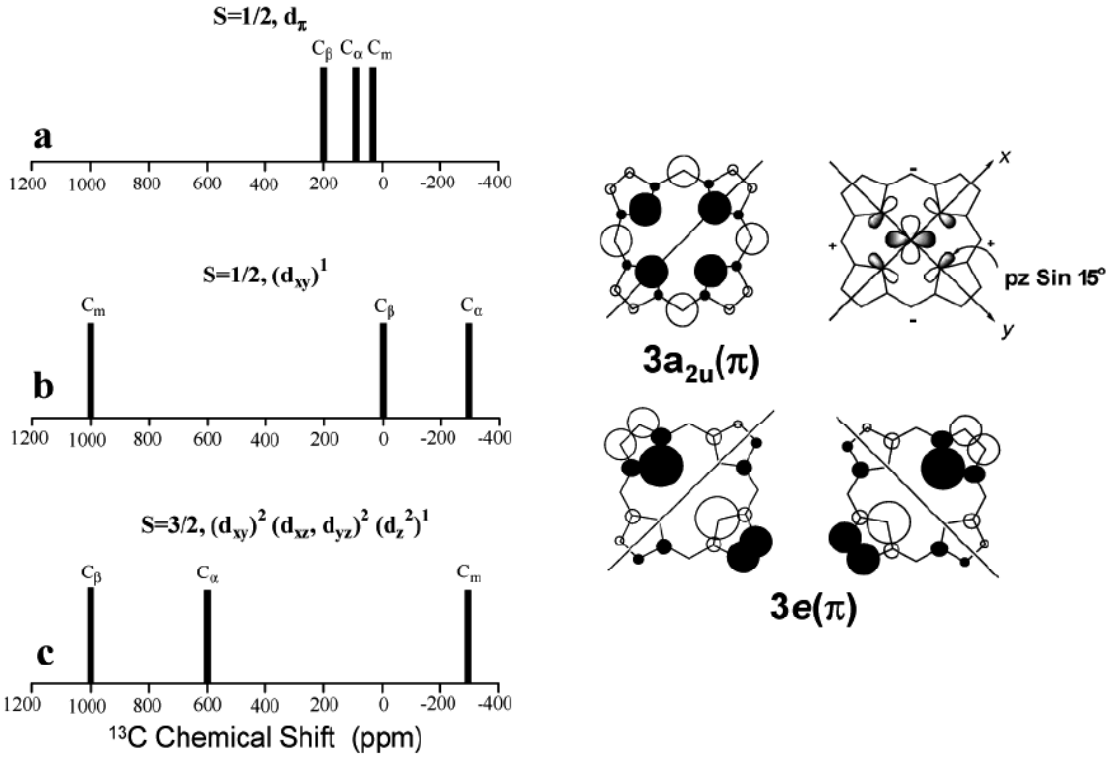

Researchers conducting the study on Heme Oxygenase used the data in Figure I.3 as a tool for characterizing the spin states, and electronic configurations of their Fe^{III}-OH model for the ferric hydroperoxide intermediate. With this data and their own, they were ultimately able to show that the most abundant spin population exhibited a spin crossover between S = ½, (d_π) and S = 3/2 spin states. They also identified two less populated spin states that were pure S = 3/2 and S = ½, $(d_{xy})^1$ electronic configurations, and stated that the relative populations of these configurations were indicative of nonplanar deformations of the macrocycle, in particular the exocyclic vinyl groups. Finally, they

concluded that abundant spin density centered at the C_m core carbons, taken with the nonplanarity of the porphyrin ring, "primes the macrocycle to actively participate in its own hydroxylation."[7] They also stated that their conclusion was only valid if the ligand field strength of the coordinated OOH^- was modulated in a similar manner as their model system. This study is a perfect illustration of the power of ^{13}C-NMR spectroscopy in the analysis of heme containing proteins.

We would ultimately like to conduct studies such as the ones mentioned above using various cytochrome P450 enzymes. However, a fundamental problem had to be overcome for this to become a possibility. The hemoproteins analyzed in the studies mentioned above as well as the cytochrome P450 enzymes we are interested in studying contain a natural abundance of ^{13}C that is much too low to be useful for ^{13}C-NMR spectroscopy given their metal centers. The studies mentioned above used reconstitution techniques to generate proteins containing labeled prosthetic heme cofactors. Unfortunately, in cytochrome P450 enzymes, the native heme is not easily removed and reincorporated without destroying the enzyme.

We have devised an expression system that allows high levels of ^{13}C incorporation into the prosthetic heme cofactor of hemoproteins using a mutant strain of *Escherichia coli* (*E. coli*) called Hu227. This system takes advantage of the biosynthesis of the heme to achieve ^{13}C incorporation. In order to use this expression system, we needed to generate new expression vectors because ours required the presence of a T7 polymerase. Hu227 contains no T7 polymerase gene naturally, and attempts to transfect these cells with the T7 polymerase gene separately from the protein expression vector

had been unsuccessful previously. We decided to generate a new expression vector that was regulated by a lac promotor and contained the CYP102A2 gene. In the interim, we generated ^{13}C-NMR hemoprotein samples using a vector that encoded for dehaloperoxidase that was under the control of a *lac* promoter. This was to primarily serve as a model system to ensure that we could isotopically label the prosthetic heme cofactor using our expression system.

I.C. *Escherichia coli* Hu227

We used the mutant strain of *Escherichia coli* (*E. coli*) Hu227 in our expression of dehaloperoxidase due to its inability to synthesize aminolevulinic acid (ALA) naturally. This particular strain of *E. coli* contains a mutation in the hemA gene, which encodes for glutamyl-tRNA.[8] Glutamyl-tRNA is required for the biosynthesis of ALA, which is the first precursor in the biosynthesis of heme. By synthesizing several isotopomers of ^{13}C ALA and ^{15}N ALA from labeled glycine and supplying it to the Hu227 cells that are unable to produce aminolevulenic acid naturally, it was possible to achieve high-level incorporation of ^{13}C or ^{15}N into the heme of dehaloperoxidase via the biosynthetic pathway of the heme cofactor shown in Figure I.4.[4]

The biosynthesis of heme begins with the condensation of two δ-aminolevulinic acid (ALA) molecules. This step is catalyzed by ALA dehydratase enzyme, forming porphobilinogen (PBG). Next, four PBG molecules are condensed by PBG deaminase forming a 1-hydroxylmethyl bilane (HMB) intermediate. This intermediate is subsequently cyclized by uroporphyrinogen III synthase forming uroporphyrinogen III (Uro'gen). The four acetate groups on uroporphyrinogen III are selectively cleaved by

the Uro'gen decarboxylase yielding coproporphyrinogen III (Copro'gen). The propionate groups located on pyrroles I and II undergo oxidative decarboxylation by Copro'gen oxidase, yielding protoporphyrinogen IX. Subsequently, protoporphyrinogen IX oxidase carries out the oxidation of protoporphyrinogen IX by removal of six hydrogen atoms to give protoporphyrin IX. The final step in the biosynthesis of heme, which is not shown in Figure I.4, is the insertion of Fe^{2+} into the macrocycle by ferrochelatase.[9]

Figure I.4. The biosynthetic pathway of heme from [5-^{13}C] aminolevulinic acid. The highlighted atom represents ^{13}C.[4]

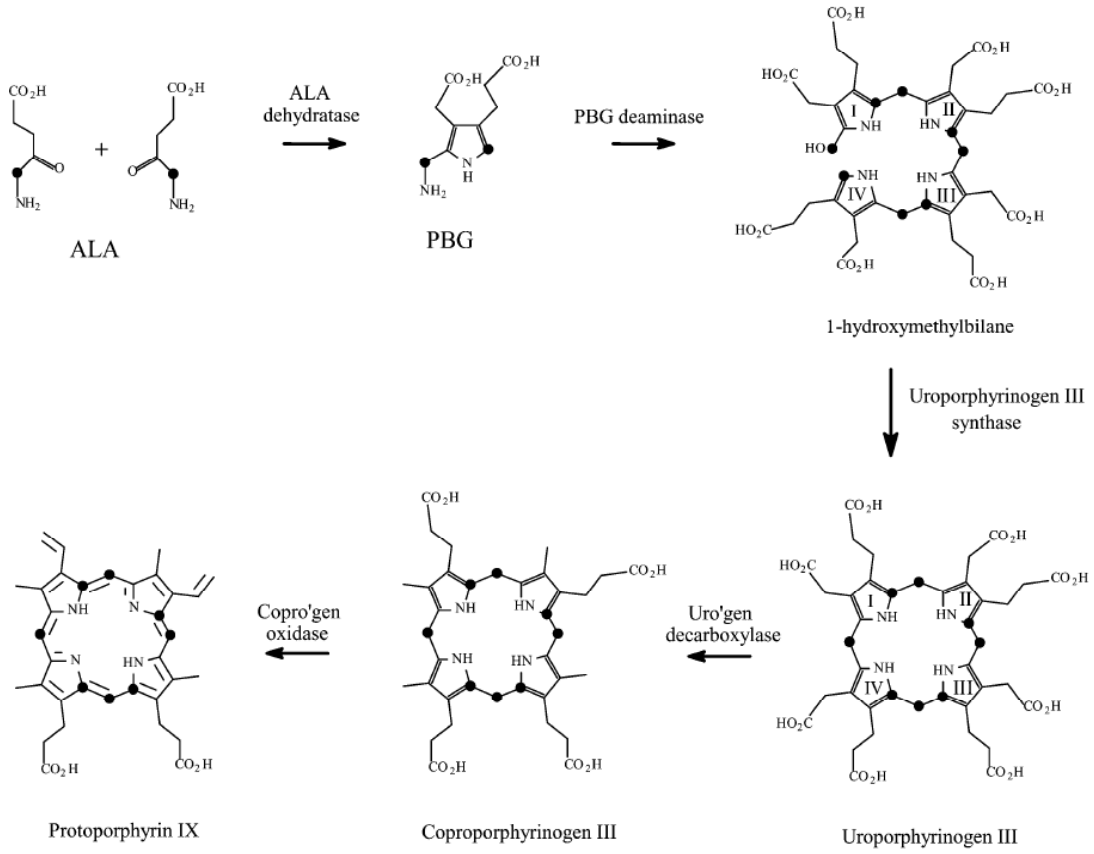

Utilizing specific isotopomers of the biosynthetic precursor ALA we can control the selective isotopic labeling of the heme cofactor. Figure I.5 shows the predicted labeling patterns generated biosynthetically from each of the three isotopomers of ALA used in our research.[4-5, 9] Starting with [4-^{13}C] ALA, only certain C_α and C_β core carbons would be isotopically labeled. No C_m core carbons should be labeled in the heme. Starting with [5-^{13}C] ALA, it can be seen in the figure that no C_β core carbons would be isotopically labeled, but all of the C_m carbons should be ^{13}C. Finally, starting with [^{15}N] ALA, a heme where only the nitrogen atoms are labeled is expected. However, before any protein with labeled heme could be expressed, the isotopomers of ALA needed to be synthesized.

Figure I.5. ^{13}C and ^{15}N labeling patterns generated when heme is biosynthesized from [4-^{13}C] ALA, [5-^{13}C] ALA, and [^{15}N] ALA.[4-5]

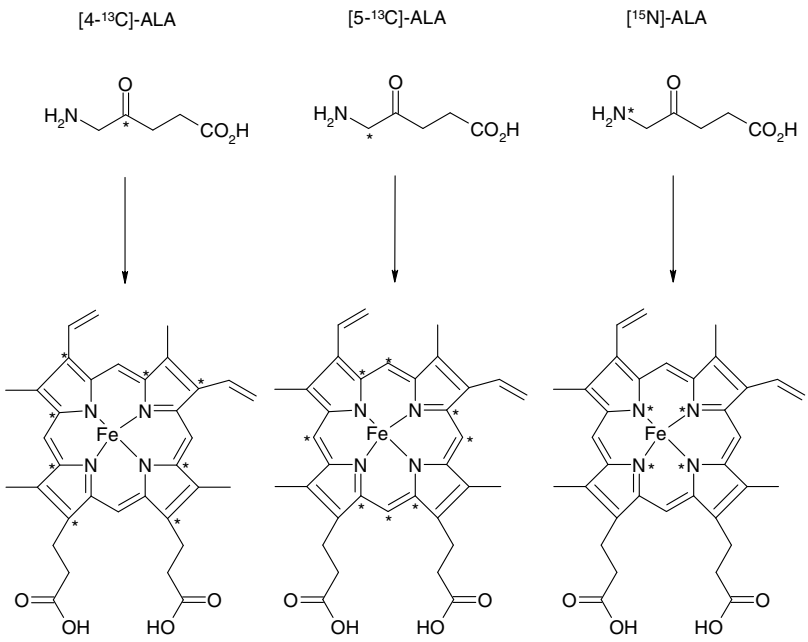

I.D. Synthesis of the isotopomers of aminolevulinic acid

The method that we chose for the synthesis of the aminolevulinic acid (ALA) isotopomers was the procedure of Wang and Scott because of the reported efficiency and economy of the four individual steps.[10] The reaction scheme for the total synthesis of ALA from the starting material glycine is shown in Figure I.6.[10] In this method, the starting material glycine is protected by phthalic anhydride in the first step followed by treatment with thionyl chloride to yield the acetyl chloride. The subsequent step in the reaction was the key step, and it required that the acetyl chloride be coupled with the zinc homoenolate using a palladium catalyst to form phthalimidolevulinic acid ethyl ester. However, before this reaction could proceed, the zinc homoenolate had to be synthesized by reacting [(1-ethoxycyclopropyl)-oxy]trimethylsilane with $ZnCl_2$ in ether. The zinc homoenolate exists as an etherate and is shown in Figure I.7.[11] Once synthesized, the zinc homoenolate of alkyl propionate can react with the carbonyl carbon of the phthalimidoacetyl chloride in a carbon-carbon bond forming reaction to yield the phthalimidolevulinic acid ethyl ester. Deprotection can then proceed by the acid hydrolysis of phthalimidolevulinic acid ethyl ester with hydrochloric acid to yield the final product, ALA. In this synthesis [1-^{13}C] glycine may be used as the starting material to ultimately generate [4-^{13}C] ALA, [2-^{13}C] glycine can be used to generate [5-^{13}C] ALA, and [^{15}N] glycine can be used to generate [^{15}N] ALA.

Figure I.6. The synthetic procedure for the generation of unlabeled ALA, [4-^{13}C] ALA, [5-^{13}C] ALA, and [^{15}N] ALA.[10]

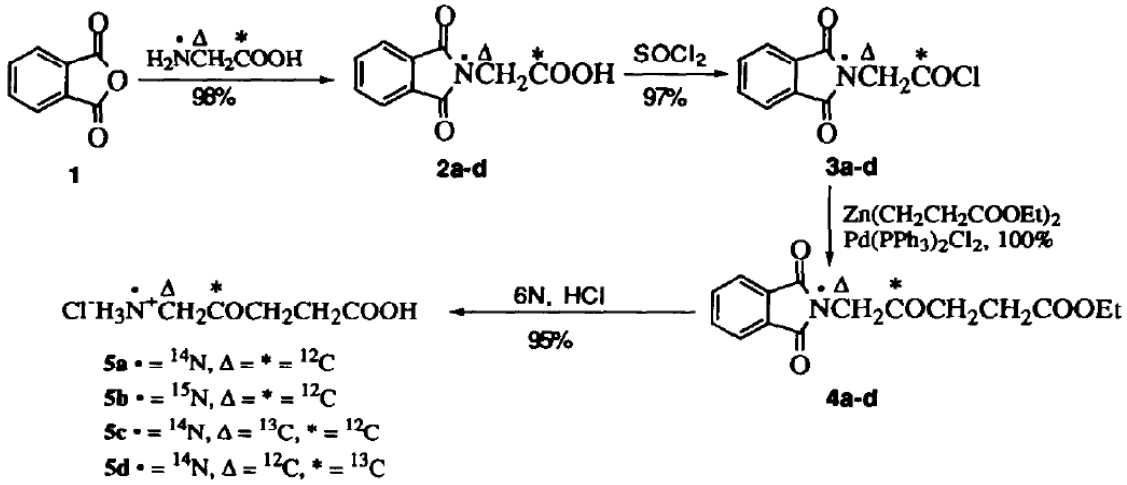

Figure I.7. Synthesis of zinc homoenolate.[11]

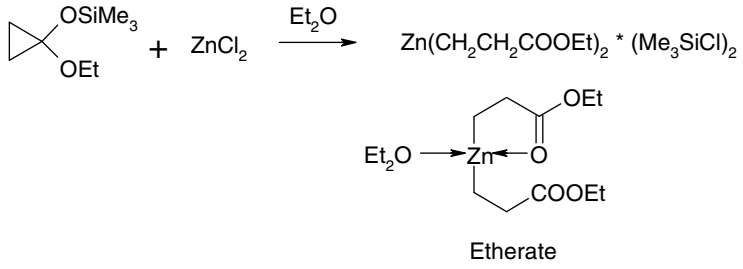

I.E. Dehaloperoxidase

Selection of dehaloperoxidase (DHP) for these studies was based on the availability of an effective expression vector for this moderately sized hemoprotein (~31 kDa)[12] that was under the control of a *lac* promoter. *Amphitrite ornate* is a polychaete worm that has the capability of surviving in estuarine mud flats that are

contaminated with halophenols. Although such compounds have been widely dispersed by humans, and constitute a significant environmental problem, these compounds are also generated as a sort of chemical warfare by other marine organisms.[13-15] Enzymes involved in the breakdown of halophenols would be appealing to study for the purpose of bioremediation. DHP is the globular heme-containing enzyme that provides this marine worm with its unique ability of catalyzing the oxidative dehalogenation of noxious halogenated phenols in the reaction shown in Figure I.8.[16] It can also be seen in the figure that H_2O_2 is required to catalyze the dehalogenation of the trihalogenated phenols, but DHP is also capable of oxidizing mono- and dihalogenated phenols as well, which are not shown.[13, 15]

Figure I.8. Reaction catalyzed by dehaloperoxidase of *Amphitrite ornate*.[16]

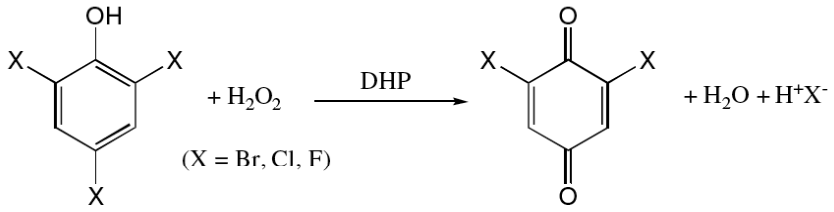

In recent studies using UV-Visible absorption and magnetic circular dichroism, it has been demonstrated that exogenous ligand-free ferric DHP is hexa-coordinate with a distal water and a proximal neutral histidine as axial heme ligands.[16] This coordination state is distinct from other ferric resting state histidine ligated peroxidases, which activate peroxide through a mechanism involving an electronic push-effect initiated by a partially

ionized proximal histidine ligand. We have successfully incorporated ^{13}C into a variety of different positions in the heme of DHP using a recombinant expression system, and have also been able to incorporate ^{15}N into the heme as well. With these samples, future studies using ^{13}C-NMR and ^{15}N-NMR should be possible in order to characterize the coordination state of the exogenous ligand-free ferric resting state of DHP. This would further demonstrate the power and validity of this method in the characterization of heme coordination states. Perhaps more importantly, we can also use these samples to probe the electronic configuration of the heme in various oxidation states. Studies of the electronic configurations of the heme are not accomplished in a simple fashion by any other method, and to our knowledge no such studies have been conducted on this particular enzyme.

I.F. Cytochrome $P450_{102A2}$

While attempting to generate dehaloperoxidase containing a labeled heme, a separate project was also underway where we were ultimately able to clone the CYP102A2 gene of *Bacillus subtillis* 168 (*B. subtillis*). The P450 CYP102A2 is one of eight P450s encoded by *B. subtillis*.[17, 25] Additionally, CYP102A2 is a homolog of CYP102A1, which is the flavocytochrome P450 BM3 encoded by *Bacillus Megaterium*. CYP102A2 also shares the rare characteristic of containing each of the cofactors flavin adenine dinucleotide (FAD), flavin mononucleotide (FMN), and heme. It has also been demonstrated that this enzyme binds and catalyzes the hydroxylation of a range of long-chain fatty acids.[18-20]

Keeping in mind that we wanted to be able to express the CYP102A2 in Hu227 cells, we followed a modified version of the cloning method described by Gustafsson et al.[17] This procedure required the ligation of the CYP102A2 gene into the pBluescript II SK(-) vector (Stratagene), which is shown in Figure I.9.[21] It can be seen from the vector map in the figure that the multiple cloning site is under the control of a *lac* promoter, which eliminated the need for a T7 polymerase. Therefore, cloning into this vector made CYP102A2 expression more compatible with our Hu227 cells. In future studies, the compatibility will allow us to eventually overexpress the CYP102A2 with isotopically labeled heme for ^{13}C-NMR studies as discussed earlier. The optimization of growth conditions for the enzyme in our expression system would need to be worked out using unlabeled aminolevulinic acid prior to any experiment using the more expensive isotopomers of the aminolevulinic acid.

Figure I.9. Vector map and sequences of pBluescript II SK (-).[21]

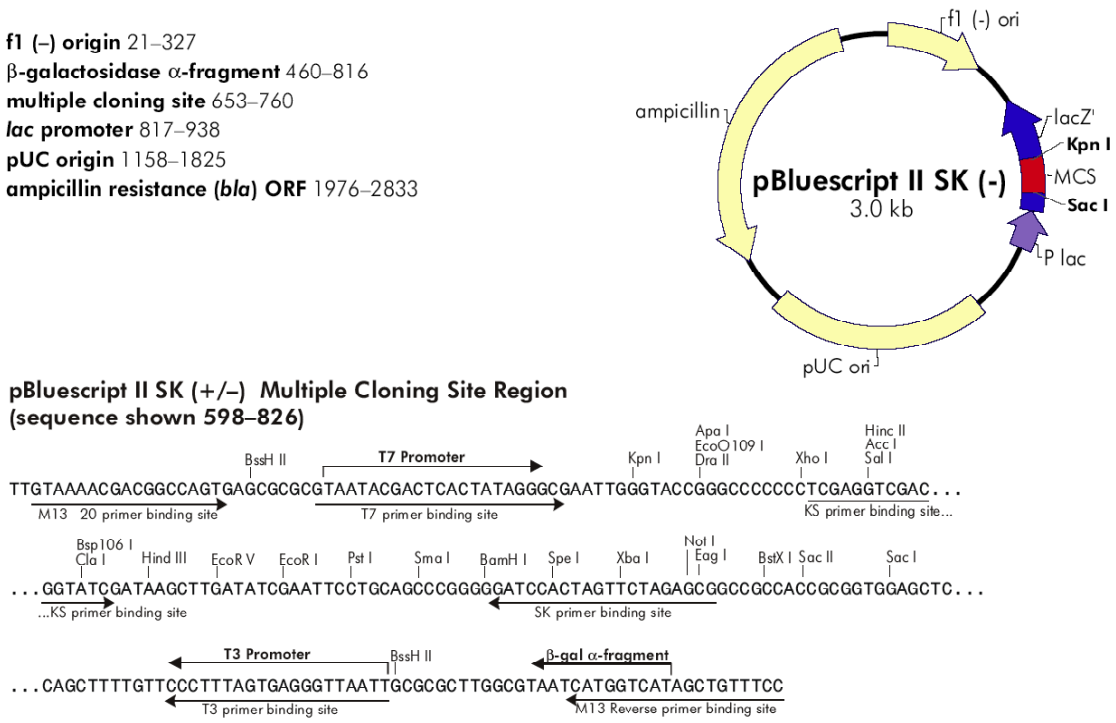

In the current study, our goal was to be able to express and purify the CYP102A2 enzyme from Hu227 cells after cloning was accomplished. Then we wanted to assay its activity towards the substrate *p*-Nitrophenoxydodecanoic acid (12-pNCA). We followed the method described by Schwaneberg et al., where the NADPH dependent hydroxylation of 12-pNCA by the P450 was monitored via product formation spectrophotometrically.[18] Figure I.10 displays the reaction that is catalyzed by the CYP102A2 homologue P450 BM-3 F87A.

Figure I.10. Reaction scheme of *p*-nitrophenoxycarboxylate (pNCA) conversion by P450 BM-3 F87A. The formation of *p*-nitrophenolate is monitored at 410 nm.[18]

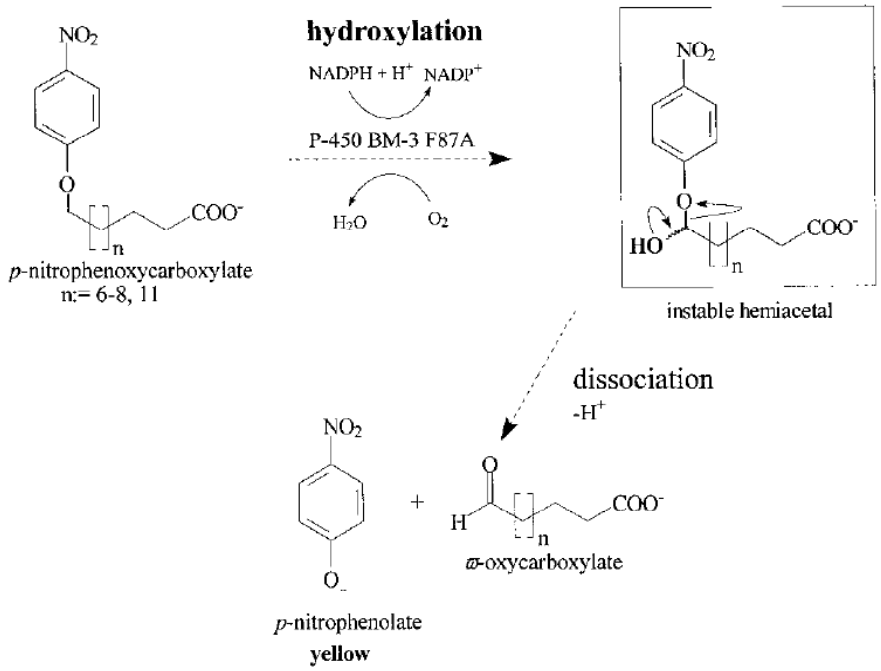

In this research project, we were able to successfully synthesize and characterize three isotomomers of aminolevulinic acid (ALA): [4-^{13}C] ALA, [5-^{13}C] ALA, and [^{15}N] ALA. These three isotopomers were used in the expression of the hemoprotein dehaloperoxidase (DHP) in *E. coli* Hu227 cells, which were incapable of synthesizing their own ALA. We were able to show through analytical techniques, that high levels of ^{13}C and ^{15}N were incorporated into the heme of DHP. We also generated a CYP102A2 expression vector that was under the control of a *lac* operon. This was done in order to create a P450 expression vector that was compatible with our expression system. This will enable future heme labeling studies to be performed on this enzyme. Overexpression of the generated CYP102A2 expression vector was accomplished in *E. coli* Hu227 cells,

and an activity assay was conducted with the enzyme and 12-*p*-nitrophenoxycarboxylic acid.

CHAPTER II

EXPERIMENTAL

II.A. Synthesis of ^{13}C and ^{15}N δ-aminolevulinic acid (ALA) isotopomers

[1-^{13}C] glycine, [2-^{13}C] glycine, and [^{15}N] glycine were purchased from Cambridge Isotope Laboratories, Inc. All other chemicals used were obtained from Aldrich, Fisher Scientific, Acrōs, and Pharmco. [4-^{13}C] Aminolevulinic acid (ALA), [5-^{13}C] ALA, and [^{15}N] ALA were each prepared via the synthetic procedure described by Wang and Scott [10]. Only the starting material glycine was varied in each case; [1-^{13}C] glycine was used in the synthesis of [4-^{13}C] ALA, [2-^{13}C] glycine was used in preparing [5-^{13}C] ALA, and [^{15}N] glycine was used in the synthesis of [^{15}N] ALA. Moisture sensitive reactions were always carried out under an atmosphere of nitrogen or argon gas, and moisture sensitive liquid reagents were always delivered to reactions via syringe. Only round bottom flasks and medium length condensers with 14/20 joints were used during reactions to prevent excessive loss of solvents. Diethyl ether was kept dry in a solvent purification system, and was used immediately after being dispensed. Characterization of products was done using nuclear magnetic resonance spectroscopy, and was carried out on a JEOL JNM-ECA500 FT NMR system. The mole values, reaction yields and NMR data given in this procedural section, in order to avoid confusion, are for reagents and products in the synthesis of [5-^{13}C] ALA.

II.A.1 Isotopomers of phthalylglycine

[2-^{13}C] glycine (99 atom% ^{13}C, 1.010 g, 13.28 mmol) was reacted with phthalic anhydride (1.992 g, 13.45 mmol) in a 50 mL round bottom flask using indirect heat over a Bunsen burner with gentle swirling under a stream of dry argon gas. Heating caused the white powders to liquefy and simmer lightly until solid crystals began forming on the inner sides of the flask. Heating was continued for 2 minutes after solids began forming. The resulting off-white solid was recrystallized from water, yielding [2-^{13}C] phthalylglycine as white needles (2.470 g, 90.2%); ^{1}H-NMR (DMSO) δ 4.28 (d, ^{1}J = 141.8, 2H, $^{13}CH_2CO$), 7.88 (AA'BB', 4H, H-Ph). Product was dried in an oven at 100 ^{o}C and stored in a desiccator at room temperature.

II.A.2 Isotopomers of phthalimidoacetyl chloride

Dried, [2-^{13}C] phthalylglycine (2.388 g, 11.58 mmol) was refluxed for 18 hours in thionyl chloride (12.0 mL, 165.2 mmol) in a 25 mL round bottom flask equipped with a Teflon coated magnetic stir-bar and a reflux condenser. The reaction proceeded under continuous argon gas flow in an 80 ^{o}C oil bath. The resulting orange liquid was allowed to cool, and thionyl chloride was removed with a BÜCHI Rotovapor R-200. Excess thionyl chloride was removed from the resulting dried yellow solid by dissolving in dry diethyl ether and evaporating the solvent (2 x 10 mL), which left [2-^{13}C] phthalimidoacetyl chloride behind as a yellow powder (2.557 g, 98.3%); ^{1}H-NMR ($CDCl_3$) δ 4.82 (d, ^{1}J = 146.3, 2H, $^{13}CH_2CO$), 7.85 (AA'BB', 4H, H-Ph). The acid chloride was stored at room temperature for up to two weeks.

II.A.3 Isotopomers of phthalimidolevulinic acid ethyl ester

The next step required the synthesis of zinc homoenolate to be used in a subsequent reaction with the phthalimidoacetyl chloride. Zinc chloride (2.046 g, 15.01 mmol) was fused in a 100 mL round bottom flask under vacuum with indirect heat over a Bunsen burner. This was allowed to cool under vacuum to a white solid and was used immediately. Next, the zinc chloride was stirred at room temperature under argon gas flow in dry diethyl ether (30 mL) in the 100 mL flask equipped with a reflux condenser. Once a clear homogenous mixture was obtained, dry [(1-ethoxycyclopropyl)-oxy]trimethylsilane (6.0 mL, 30 mmol) was added to the reaction drop wise with a syringe over a 5-minute period to give a cloudy solution. Stirring continued at room temperature for 1 hour followed by refluxing in a hot oil bath for 30 minutes to generate the crude zinc homoenolate.

The zinc homoenolate solution was stirred in an ice water bath under an atmosphere of argon gas. Tetrakis(triphenylphosphine)palladium(0) (148 mg, 0.128 mmol) and [2-^{13}C] phthalimidoacetyl chloride (2.413 g, 10.74 mmol) were added to the stirring solution all at once. Once a homogenous mixture was obtained, N, N-dimethylacetamide (3 mL, 32 mmol) was added slowly via syringe. These components were allowed to stir at 0 ^{o}C under argon gas flow for 1 hour and continued stirring at room temperature for 2 hours.

This mixture was evaporated down to a light brown residue, and was then dissolved in 100 mL of dichloromethane. The solution was transferred to a 250 mL separatory funnel and was washed with 50 mL of water to quench the reaction. The

aqueous fraction was discarded and the dichloromethane was washed with 50 mL of water saturated with NaCl. The organic fraction was saved and dried overnight over sodium sulfate in a 125 mL Erlenmeyer flask capped with a rubber septum. The clear orange solution was evaporated down to a deep orange colored solid under vacuum. This was recrystallized from ethanol to yield the [5-^{13}C] phthalimdolevulinic acid ethyl ester as light yellow crystals (2.706 g, 90.5%); ^{1}H-NMR ($CDCl_3$) δ 1.25 (t, ^{3}J = 7.4, 3H, $OCH_2C\underline{H}_3$), 2.65 (t, ^{3}J = 6.7, 2H, $COCH_2C\underline{H}_2$), 2.84 (t, ^{3}J = 6.4, 2H, $COC\underline{H}_2CH_2$), 4.14 (q, ^{3}J = 7.3, 2H, $OC\underline{H}_2CH_2$), 4.55 (d, ^{1}J = 139.3, 2H, $^{13}CH_2CO$), 7.80 (AA'BB', 4H, H-Ph).

In some cases, it was not possible to evaporate the crude product sufficiently enough to generate a dried solid. This was due to excess N, N-dimethylacetamide. In these cases, the evaporated crude product was applied to a large flash column. The desired product was separated from impurities with a 1:1 mix of ethyl acetate:hexane and the eluent was collected in several fractions. Fractions containing the labeled phthalimidolevulinic acid ethyl ester were identified using thin layer chromatography. The fractions containing the desired product were pooled and evaporated down to a yellow solid. This was washed several times with chloroform to remove excess ethyl acetate. This provided sufficiently pure product, and further recrystallization was not necessary.

II.A.4 Isotopomers of δ-aminolevulinic acid

[5-^{13}C] aminolevulinic acid was produced from the acid hydrolysis of [5-^{13}C] phthalimidolevulinic acid ethyl ester. [5-^{13}C] Phthalimidolevulinic acid ethyl ester (2.662

g, 9.57 mmol) was placed in a 50 mL round bottom flask and was refluxed overnight in a 1:1 mix of hydrochloric acid: acetic acid at 120 ^{o}C. The resulting deep yellow solution was evaporated to dryness. The resulting solid was washed with 20 mL of water to remove excess acid and an off-white solid was left behind after evaporation. This was taken up in 40 mL of water and was transferred to a 125 mL separatory funnel. The aqueous fraction was washed with (4 x 25 mL) ethyl acetate to remove phthalic acid. The aqueous fraction was saved and concentrated down to a brown oily residue with evaporation under vacuum. Finally, labeled aminolevulinic acid (ALA) was recrystallized from ethanol and diethyl ether. This was done by dissolving the ALA in hot ethanol in a round bottom flask. The solution was placed on ice, and cold diethyl ether was added drop-wise until white solid crystals of ALA precipitated out of solution; (1.506 g, 93.3%) ^{1}H-NMR (D_2O) δ 2.53 (t, ^{3}J = 6.2, 2H, $COCH_2C\underline{H}_2$), 2.73 (, 2H, $COC\underline{H}_2CH_2$), 3.95 (d, ^{1}J = 143.3, 2H, $^{13}CH_2CO$). Isotopomers of ALA were stored separately at –20 ^{o}C in brown glass vials. The overall yield was 67.2%.

II.B. Agar plate preparation: for growth of *E. coli* and expression of recombinant proteins

Agar components included 5 g of tryptone, 5 g of NaCl, 2.5 g of yeast extract, and 7.5 g of agar. These components were poured into a 1000 mL Erlenmeyer flask and equipped with a magnetic stir bar. Deionized water was added and stirred to mix the components on a tabletop magnetic stirrer. The pH was adjusted to 7.4 with 1M NaOH, and the solution was brought up to a final volume of 500 mL with additional deionized water. The Erlenmeyer flask was covered with aluminum foil and was autoclaved for 16

minutes. The hot agar solution was placed back on the tabletop magnetic stirrer, and was allowed to cool while stirring until the outside of the flask was just warm to the touch. When required, ampicillin trihydrate 50 mg (0.1 g/L) and aminolevulinic acid 10 mg (0.02 g/L) were added using sterile techniques and stirred to homogeneity. This solution was then used to fill sterile culture plates. The filled plates were covered and allowed to cool to room temperature to harden the agar. The plates were stored at 4 ^{o}C for up to four weeks.

II.C. Preparation of Luria-Bertani (LB) broth

LB broth components included 10 g of tryptone, 10 g of NaCl, and 5 g of yeast extract. These components were poured into a 1000 mL beaker and equipped with a magnetic stir bar. Deionized water was added and stirred to dissolve the components on a magnetic stirrer. The pH was adjusted to 7.4 with 1 M NaOH, and the final volume was brought up to 1000 mL with additional deionized water. The solution was further mixed to homogeneity and transferred to a 2.8 L Fernbach flask. This flask was covered with aluminum foil and then autoclaved for 16 minutes. The LB broth was then cooled to room temperature. When required, each liter of cooled broth received 0.100 g of ampicillin trihydrate and 0.020 g of appropriately labeled aminolevulinic acid. The flask remained covered with aluminum foil after addition of ampicillin and aminolevulinic acid. LB broth was used within three days after preparation.

II.D. Preparation of Terrific Broth (TB)

TB broth components included 12 g of tryptone, 24 g of yeast, and 4 mL of glycerol. These components were poured into a 1000 mL beaker and equipped with a

magnetic stir bar. Deionized water was added and stirred to dissolve the components on a magnetic stirrer. The final volume of the solution was brought up to 900 mL, and further mixed to homogeneity. This solution was transferred to a 2.8 L Fernbach flask and was covered with aluminum foil.

Phosphate buffer was prepared separately by weighing out 2.32 g of monobasic potassium phosphate, and 16.43 g of dibasic potassium phosphate. These masses were then transferred to a 125 mL Erlenmeyer flask. Next, the potassium salts were dissolved in deionized water, and the final volume was brought up to 100 mL with additional deionized water. Finally, the flask was covered with aluminum foil.

The aluminum foil covered 2.8 L Fernbach flask and 125 mL Erlymeyer flask were both autoclaved for 16 minutes. These two components were allowed to cool to room temperature, and the 100 mL of phosphate buffer was added to the 900 mL solution in the Fernbach flask. The Fernback flask was immediately covered with the sterile aluminum foil. It is important to keep the phosphate buffer separate from the other components while autoclaving and cooling in order to prevent the formation of precipitates. When required, each liter of cooled broth received 0.100 g of ampicillin trihydrate and 0.020 g of appropriately labeled aminolevulinic acid. Antibiotics and aminolevulinic acid were only added in the moments prior to inoculation, and the flask remained covered with aluminum foil after addition of ampicillin and aminolevulinic acid. TB broth was used within 3 days after preparation.

II.E. Preparation of competent HU227, HB101, and XL1-Blue cells

Escherichia Coli HU227, HB101, and XL1-Blue cells were made competent separately, using the same method. Sterile techniques were used throughout these preparative steps. Frozen stock cells were used to inoculate 25 mL of sterile LB broth contained in a 50 mL Falcon tube using a sterile wooden stick. When preparing competent HU227 cells, less than 1 mg of unlabeled aminolevulinic acid was also added to the inoculated growth media. The Falcon tube was then placed on its side in a New Brunswick Scientific C24 Incubator Shaker overnight, shaking at 240 rpm and 37 ^{o}C. The next day, 20 µl of the overnight culture was used to inoculate another 25 mL of LB media, and unlabeled aminolevulinic acid was added in the case of HU227 cells. This Falcon tube was placed in the shaker at the same settings and incubated for 4 to 5 hours with shaking. Next, 6 mL of the culture was transferred to a sterile, 15 mL Falcon tube, and was centrifuged at 5,000 rpm, for 12 minutes at 4 ^{o}C (these settings were used at each centrifuge step). The supernatant was discarded and the pellet was resuspended into 2 mL of ice cold, sterile 100 mM $MgCl_2$. After five minutes of incubation on ice, the cells were centrifuged again. The supernatent was discarded and the cells were resuspended in 2 mL of ice cold, sterile 100 mM $CaCl_2$. Cells were then incubated on ice for 45 minutes. The suspension was centrifuged again and decanted. Finally, the pellet was resuspended in 1 mL of ice cold, sterile 85 mM $CaCl_2$ with 15% glycerol. This suspension was kept on ice and was used immediately for transformations.

II.F. Transformation of *E. coli* Hu227, HB101, and XL1-Blue cells

First, 200 μl of freshly made competent cells were transferred to a sterile 1.5 mL microfuge tube that had been chilled on ice, followed by the addition of 5 μl of the plasmid to be transformed into the cells. The microfuge tube was gently tapped several times to mix, and the tube was immediately placed back on ice for 10 minutes. Next, the microfuge tube was transferred to a water bath at exactly 42 ^{o}C, and was allowed to incubate for exactly 1 minute. After incubation the microfuge tube was replaced on ice for an additional 2 minutes. Finally, 800 μl of ice cold, sterile LB broth containing no antibiotics was added to the microfuge tube.

The microfuge tube was placed in a New Brunswick Scientific C24 Incubator Shaker for between 1 and 2 hours, shaking at 240 rpm and 37 ^{o}C. Next, 100 μl aliquots of the cell suspension were spread onto LB agar plates, which contained ampicillin in the case of XL1-Blue and HB101 cells. Growth plates required both ampicillin and unlabeled aminolevulinic acid in the case of HU227 cells. The inoculated plates were incubated in an oven at 37 ^{o}C overnight, or until colonies were formed.

II.G. Expression of dehaloperoxidase with isotopically labeled heme in HU227 cells

A single colony was picked from a LB plate containing HU227 cells, which had been transformed the previous day with a stock plasmid encoding for the dehaloperoxidase (DHP) gene that was under control of a *lac* promoter. The colony was picked from the plate under sterile conditions using a sterile stick, and the colony was used to inoculate 25 mL of LB broth in a 50 mL Falcon tube containing ampicillin and unlabeled aminolevulinic acid. This tube was placed on its side in a New Brunswick

Scientific C24 Incubator Shaker overnight, shaking at 240 rpm and 37 ^{o}C. The next day, 250 μL aliquots of the overnight culture were used to inoculate four separate 2.8 L Fernbach flasks containing 1 L of LB broth. Ampicillin trihydrate and either [4-^{13}C] ALA, [5-^{13}C] ALA, or [^{14}N] ALA had been added to each flask of LB broth after sterilization of the media as explained previously. Each liter of inoculated broth was covered with aluminum foil and was placed in a New Brunswick Scientific C25KC Incubator Shaker and incubated at 24.5 ^{o}C with shaking at 207 rpm. Shaking continued for two days or until a 1 mL aliquot of culture had an A_{600} equal to 1.7 or greater. Cultures were also tested for expression of DHP using UV-Vis spectrophotometry. Protein was harvested from cultures displaying expression.

II.H. Dehaloperoxidase harvest and protein purification

Cell cultures testing positive for DHP over-expression were transferred to 500 mL centrifuge tubes. The cultures were centrifuged in a Beckman Avanti J-25 centrifuge at 9,500 rpm at 4 ^{o}C for 30 minutes using a JA 10 Beckman rotor. The supernatant was discarded, and the pellet was resuspended and homogenized in 100 mL of pH 5.0, 50 mM phosphate equilibration buffer. Cell walls were lysed with lysozyme for 20 minutes at room temperature while stirring. The lysed cells were transferred to 40 mL centrifuge tubes and the membranes were degraded by sonication using a Fisher Scientific 60 Sonic Dismembrator while on ice, in four 30-second bursts, and at a power of 20W. The 25 mL centrifuge tubes were transferred to a JA-20 Beckman rotor and centrifuged at 19,000 rpm for 30 minutes at 4 ^{o}C. Supernatant containing the DHP was decanted and saved, while the cell fragments were discarded. DHP concentration was determined by UV-Vis

spectrophotometry of the CO-reduced heme of DHP, and the crude protein was then stored at -80 ^{o}C or immediately purified.

Next, the pH of the cell-free extract was readjusted to 5.0 by adding 1M HCl drop-wise. The crude protein was transferred to 40 mL centrifuge tubes and centrifuged again in a JA-20 Beckman rotor under the previous conditions. The supernatant was passed through a purification column containing Whatman pre-swollen DE52 diethylaminoethyl cellulose that had been equilibrated previously using about 5 column volumes of 50 mM phosphate buffer at pH 5.0. DHP passed through the purification column in a chromatography refrigerator at 4 ^{o}C, and impurities bound to the solid phase through electrostatic interactions.

The flow-through was collected and transferred to a Millipore Stirred Ultrafiltration Cell 8200 equipped with a Millipore Ultrafiltration Membrane YM1 (NMWL:1 kDa). The protein sample was concentrated down to a final volume of 15 mL while stirring in the refrigerator at 4 ^{o}C. The sample was further concentrated down, at 4 ^{o}C, to a volume of 2 mL using a Millipore Centriprep YM-3 (NMWL:3kDa) in a Fisher Scientific Centrific Centrifuge spinning at 4,000 rpm.

The 2 mL of concentrated crude DHP was further purified by size exclusion chromatography using a Sephacryl S200 (Pharmacia) column. The column had been equilibrated previously using 800 mL of 50 mM phosphate buffer at pH 5.0, and the DHP sample was run through at 4 ^{o}C. The protein moved through the column as a tight dark red or brown band. The protein was collected in 2 to 3 mL fractions as it eluted.

Collected protein fractions were tested for purity of DHP by spectrophotometry without further treatment using a Varian CARY 100 Bio UV-Visible Spectrophotometer. The samples were scanned from 250 nm to 500 nm in baseline subtraction mode against water. Fractions that contained an absorbance ratio of 1:3, at 280 nm and 418 nm respectively, were concentrated to at least 0.2 mM, which was determined by the CO-reduced spectrum of DHP. Enough glycerol was added to the concentrated, pure DHP samples to yield a 10% glycerol final concentration before freezing the samples in a -80 ^{o}C freezer. Impure fractions were stored separately at -20 ^{o}C to be used for heme extractions at a later time.

Lastly, all purification columns were washed with about 4 column volumes worth of 20% ethanol after each protein purification procedure in order to clean the columns of impurities and residual protein. These washing were collected and saved separately at -20 ^{o}C according to the labeled heme content. These washings were used at a later time for heme extractions.

II.I. DHP assay via UV-Vis spectrophotometry of the CO-reduced heme

The concentration of DHP in Hu227 cells was found using a variation of the method described by Omura and Sato[22] for detection of the hemoprotein, cytochrome P450. The extinction coefficient was assumed to be ε_{418}= 193 mM^{-1} cm^{-1}, and the concentration of DHP was determined from the absolute spectra of the reduced CO complex.[27]

The DHP concentration in intact cells was determined by centrifuging a 2 mL aliquot of cultured cells from the Fernbach flask in a Fisher Scientific Centrific

Centrifuge spinning at full speed for 10 minutes at 4 ^{o}C. The growth broth was discarded by decanting and the cell pellet was resuspended in 2 mL of 50 mM phosphate buffer at pH 7.4. One quartz cuvette was filled with deionized water and placed in the sample compartment of a Varian CARY 100 Bio UV-Visible Spectrophotometer. A baseline spectrum was recorded on the deionized water from 400 nm to 500 nm. Next, approximately 5 mg of sodium dithionite (Sigma) was dissolved in the 2 ml cell suspension to reduce the prosthetic heme iron of DHP. Carbon monoxide gas was slowly bubbled through the cell suspension for one minute to form the reduced heme iron-CO complex, and 1 mL was transferred to another quartz cuvette. The water filled cuvette was transferred to the reference compartment of the spectrophotometer, and the cuvette containing the cell suspension was placed in the sample compartment. The absorbance spectrum of the reduced CO complex of DHP was recorded from 400 nm to 500 nm with the baseline subtracted. The reduced heme iron-CO complex of DHP absorbed at 418 nm.

The DHP concentration in crude, cell-free extract was determined by diluting a 100 μL aliquot of the extract up to 1 mL with 50 mM phosphate buffer at pH 5.0. Next, the sample was gently bubbled with carbon monoxide for 1 minute, followed by the addition of a few grains of sodium dithionite. The spectrum of the reduced heme iron-CO complex of DHP was then recorded from 400 nm to 500 nm with a baseline spectrum of deionized water subtracted. The procedure for finding the concentration of DHP in concentrated, purified samples was identical to that of the crude extract except that a 10 μL aliquot of purified sample was diluted up to 1 mL in this assay.

II.J. Preparation of dehaloperoxidase for ^{1}H and ^{13}C NMR

NMR samples of DHP, which had been overexpressed in growth media containing [5-^{13}C] aminolevulinic acid, were prepared using 1 μmole of the hemoprotein. The protein was concentrated down to about 2 mL with a Millipore Centriprep YM-3 (NMWL:3kDa), in a Fisher Scientific Centrific Centrifuge spinning at 4,000 rpm. Potassium ferricyanide was added (100 μmole) to oxidize all heme iron in the protein sample. The 2 mL sample was applied to a desalting column (Sephacryl S200 by Pharmacia) that had been equilibrated with four column volumes of 50 mM phosphate buffer at pH 5.0. The brown protein separated well from the bright yellow complex salt. The oxidized protein fraction was saved and concentrated to 1 mL. Next, the aqueous phosphate buffer was exchanged with 50 mM phosphate at pH 5.0 in D_2O. This was accomplished by a 1:6 dilution of protein to phosphate buffer in D_2O, followed by concentrating the sample. This was repeated twice more to bring the theoretical concentration of H_2O in the sample down to less than 0.5%.

II.K. Extraction and purification of labeled prosthetic heme from dehaloperoxidase

Heme extractions from DHP were conducted using a variation of the method described by Teale and Yonetani[23,24]. ^{13}C and ^{15}N labeled heme samples from DHP were obtained by first thawing the 20% ethanol column washings as well as the impure size exclusion column fractions. These samples were pooled according to the labeled heme content. Next, the pH was adjusted to 2.0 with 1 M HCl in order to denature protein and release heme into solution. The resulting pink slurry was divided into glass test tubes, and equal volumes of butanone were added to each tube to pull free heme out of the aqueous

phase. The tubes were shaken vigorously for about a minute and then centrifuged at 4 ^{o}C for 45 minutes in a Fisher Scientific Centrific Centrifuge spinning at 8,000 rpm. After centrifugation, the organic layer containing the heme was pulled off of the separate aqueous phase. The addition of butanone, followed by shaking and centrifugation was repeated on the aqueous phase (2x).

Next, the butanone fraction was lyophilized, and dried crude heme was dissolved in a small amount of methanol. The solution was then diluted with water to bring the methanol concentration down to 30%. Additionally, enough glacial acetic acid was added to the solution to yield about a 0.1% concentration. This 30% methanol solution was passed through a pre-equilibrated Sep-Pak C18 3cc column (Waters) in order to apply the labeled heme to the solid phase. About 10 mL of additional 30% methanol with 0.1% acetic acid was passed through the column after the application of heme. Finally, a concentrated brown band of heme was eluted using methanol. The methanol was lyophilized to leave a dried heme sample. These dry samples were stored in the freezer at -20 ^{o}C until they were used for preparing NMR and MALDI-TOF samples.

II.L. Preparation of isotopically labeled heme samples for NMR analysis

Dry heme samples were removed from the freezer, and were washed and dried from a few milliliters of pyridine several times to ensure that all of the methanol was removed. The dried sample was taken up in pyridine-d5 (Cambridge Isotope Laboratories, Inc.), and an equimolar amount of stannous chloride was added in order to insure that all heme was reduced in the sample. Samples were then ready for NMR analysis.

II.M. Preparation of heme samples for MALDI-TOF analysis

Dry heme samples were removed from the freezer, and were each diluted up to 100 μL with methanol. These solutions were used to make 1:10 and 1:100 dilutions in methanol to be used in the spotting solutions. The matrix used was a saturated solution of α-cyano-4-hydroxycinnamic acid in acetonitrile with 0.1% trifluoroacetic acid. Spotting solutions were prepared by adding 1 μL of sample to 12 μL of the matrix diluent, and finally a 12 μl aliquot of the matrix solution was added. A MALDI plate was spotted with 0.5 μL of this sample for analysis.

II.N. MALDI-TOF analysis of heme samples from DHP

MALDI samples were analyzed in an Applied Biosystems 4700 Proteomics Analyzer. Analysis was conducted in reflector positive mode.

II.O. Preparation of isotopically labeled heme samples for (LC-MS) analysis

Samples of isotopically labeled heme were obtained individually from purified samples of DHP. First, 20 μL of a purified DHP sample was transferred to a microfuge tube. Next, 180 μl of 0.05% acetic acid in acetonitrile was added to denature the protein and release the heme into solution. The microfuge tube was centrifuged in a tabletop microfuge for 5 minutes at 14,000 rpm. The supernatant was transferred to a high performance liquid chromatography (HPLC) glass sample vial and was placed in the autoloader of a Shimadzu HPLC system equipped with a C18 column from Stellar Phases Inc., Longhorne, PA 19047. The sample was passed through the system at a flow rate of 1 mL per minute, and the absorbance of eluent was monitored at 398 nm. The mobile phase used was a 60:40 mix of acetonitrile to water, with a 0.5% acetic acid

concentration in the final volume. The volume of flow through corresponding to the largest peak was collected as it eluted between the retention times of 8 and 10 minutes. These samples were lyophilized to dryness and were frozen at -20 ^{o}C.

II.P. LC-MS analysis of purified heme isotopomers

Dried heme samples that had been HPLC purified were taken up in 200 μl of the HPLC mobile phase mix described previously. The samples were centrifuged briefly with a tabletop centrifuge and were transferred to Target DP™ Vials C4000-1 (National Scientific Company). The samples were sealed with 9 MM Blue Caps T/S (Fisherbrand) and were injected separately into a Hewlett Packard Agilent 1100 series HPLC equipped with a 5 mM Prevail C-18 column (Alltech). Data was obtained from an LCQ Advantage Thermo Finnigan coupled with LC-MS and electrospray ionization. The mass range analyzed was from 350 to 800 daltons, and the flow rate used during analysis was 0.2 ml per minute.

II.Q. Cloning of the P450 CYP102A2 gene from *Bacillus subtilis 168*

Cloning procedures were modified from Gustafsson et al.[17] Genomic DNA from *Bacillus subtilis* (*BS*) 168 was a gift from the research lab of Dr. Jason Reddick. A polymerase chain reaction (PCR) was performed using the components and amounts listed in Table II.1. PCR primers 102A21 and 102A22 contained XbaI and XhoI restriction sites respectively and are underlined in Table II.1. PCR reactions were conducted as follows: 1 hold at 98 ^{o}C for 4 minutes; 25 cycles of 98 ^{o}C for 30 seconds, 60 ^{o}C for 30 seconds, and 72 ^{o}C for 3 minutes; 72 ^{o}C for 5 minutes. PCR product was confirmed by agarose gel electrophoresis using a 1% agarose gel containing 1 x TAE

buffer, and was purified by a Qiagen PCR purification kit. Purified PCR product was stored at -20 ^{o}C. The 1 x TAE buffer used in the 1% agarose electrophoresis gel was obtained by making dilutions of a 50 x TAE buffer stock. 50 x TAE buffer components included 242.0 g of Tris base, 57.1 mL of glacial acetic acid, and 18.6 g ethylenediaminetetraacetic acid (EDTA). These components were combined and dissolved in deionized water. The final volume was brought up to 1 L and the solution was stored at room temperature.

Table II.1. PCR reaction components and volumes for a single reaction

PCR component	**Component Volume**
Primer 1: 102A21 (5'-CCCTCTAGAGGG AGGTATGTTCGATGAAGGAAACAAGCC-3'); Integrated DNA Technologies, Inc.	1 µl
Primer 2: 102A22 (5'-CCCTCGAGTCTT CTTTATCTATATCCCTGC-3'); Integrated DNA Technologies, Inc.	1 µl
Template DNA: Genomic DNA from *B.S.* 168	1 µl
Taq Master Mix; New England Biolabs	12.5 µl
ddH_20	8.5 µl

Restriction digests were carried out on purified PCR product and the expression vector, pbluescript II SK(-). Restriction digest components are listed in Table II.2. Restriction digest reactions were carried out as follows: 1 hold at 37 ^{o}C for 2 hours; 1 hold for 65 ^{o}C for 20 minutes. Restriction digest products were confirmed by 1% low melting agarose gel electrophoresis containing 1 x TAE. Vector and PCR product digests were both purified individually by a Qiagen PCR purification kit. Digest products were stored at -20 ^{o}C.

Table II.2. Restriction digest components and volumes for four separate reactions of insert, vector, and two controls.

Digest Component	**Volume (Vector Digest)**	**Volume (PCR Product)**	**Volume (Control#1)**	**Volume (Control#2)**
1 x NE Buffer 2; New England Biolabs	2.5 µl	2.5 µl	2.5 µl	2.5 µl
Vector (pbluescript II SK(-)); Stratagene	6.0 µl	None	None	None
PCR Product (Insert)	None	10.0 µl	10.0 µl	10.0 µl
Bovine Serum Albumin (BSA); New England Biolabs	0.3 µl	0.3 µl	0.3 µ	0.3 µ
ddH_2O	14.2 µl	10.2 µl	10.2 µl	10.2 µl
XbaI restriction enzyme; Roche	1.0 µl	1.0 µl	1.0 µl	None
XhoI restriction enzyme; New England Biolabs	1.0 µl	1.0 µl	none	1.0 µl

Purified restriction digest products were used in four, 20μl ligation reactions in an attempt to generate the desired recombinant plasmid. Reaction components and volumes are listed in Table II.3. The products of all four reactions were combined and were successfully transformed into XL1-Blue cells, obtained from Stratagene, and grown on ampicillin containing Luria Bertani (LB) agar plates. Colonies that grew on the ampicillin LB plates were then screened in two steps for recombinant DNA containing insert.

Table II.3. Ligation reaction components and volumes for 4 separate reactions

Ligation Reaction Components	**Component Volumes (Reaction #1)**	**Component Volumes (Reaction #2)**	**Component Volumes (Reaction #3)**	**Component Volumes (Reaction #4)**
Purified Vector	1 μl	1 μl	1 μl	1 μl
Purified Insert	1 μl	2 μl	3 μl	6 μl
Ligation Buffer; New England Biolabs	2 μl	2 μl	2 μl	2 μl
Ligase; New England Biolabs	1 μl	1 μl	1 μl	1 μl
ddH_2O	15 μl	14 μl	13 μl	10 μl

First, several colonies were chosen from the agar plates and were grown individually overnight in LB media containing ampicillin. Plasmids were purified from the growth media using a Qiagen plasmid miniprep kit. Purified plasmids were analyzed on a 1% agarose electrophoresis gel containing 1 x TAE. The sizes of the purified plasmids were compared to uncut pbluescript II SK(-) vector and uncut CYP102A2-insert. Bands that were larger than both uncut pbluescript II SK(-) vector and uncut CYP102A2-insert suggested that ligation of insert into the pbluescript II SK(-) vector was accomplished.

The second step in screening was to test the successfully ligated plasmids from the first screen for the presence of ligated insert. This was carried out with PCR using the components and volumes included in Table II.4. PCR products were analyzed on a 1% agarose electrophoresis gel including 1 x TAE, and band sizes were compared to cut CYP102A2-insert. Band sizes that were similar to the cut CYP102A2-insert suggested that the desired insert had been ligated into the pbluescript II SK(-) vector. Plasmids containing vector were stored at –80 ^{o}C.

Table II.4. Screening PCR components and volumes for a single reaction

PCR component	**Component Volume**
Primer 1: 102A21 (5'-CCCTCTAGAGGGAGGTATGTTCGATGAAGGAAACAAGCC-3')	1 μl
Primer 2: 102A22 (5'-CCCTCGAGTCTTCTTTATCTATATCCCTGC-3')	1 μl
Purified plasmid from a single colony	1 μl
Master Mix; New England Biolabs	12.5 μl
ddH_20	8.5 μl

Large stocks of successfully ligated plasmid containing the CYP102A2 gene were generated by first transforming the plasmid into HB101 cells. The cells were then plated on LB containing ampicillin, and incubated at 37 ^oC overnight. The next day, a single colony of HB101 cells was picked from the plate and was grown overnight in 25 mL of ampicillin containing LB as described previously. This overnight culture was used to isolate the desired plasmid using a Qiagen plasmid miniprep kit. Stocks of the CYP102A2 plasmid were stored at -80 ^oC.

II.R. Expression of CYP102A2 in HU227

HU227 cells were transformed with the cloned CYP102A2 plasmid and grew overnight on a LB agar plate containing ampicillin and unlabeled aminolevulinic acid. A single colony was selected from the LB plate under sterile conditions using a sterile stick.

The selected colony was used to inoculate 25 mL of Terrific Broth (TB) in a 50 mL Falcon tube containing ampicillin and unlabeled aminolevulinic acid. This tube was placed on its side in a New Brunswick Scientific C24 Incubator Shaker overnight, shaking at 240 rpm and 37 ^{o}C. The next day, 250 µl aliquots of the overnight culture were used to inoculate 4 separate 2.8 L Fernbach flasks containing 1 L of TB broth each. Ampicillin trihydrate and unlabeled aminolevulinic acid had been added to each flask of TB in the amounts and conditions previously stated. Each liter of inoculated broth was covered with aluminum foil, placed on a New Brunswick Scientific Gio Gyrotory Shaker, and incubated at room temperature with shaking at 207 rpm. Shaking continued until a 1 mL aliquot of culture had an A_{600} equal to 2.0. Isopropyl β-D-1-thiogalactopyranoside (IPTG) was added (0.15 g/L) to initiate overexpression, and shaking continued at 70 rpm. Cultures were tested for expression of CYP102A2 using electronic absorption spectrophotometry of the CO-reduced vs reduced heme. Cells were then harvested from cultures displaying expression.

II.S. Harvest and purification of CYP102A2

Cell cultures testing positive for CYP102A2 over-expression were transferred to 500 mL centrifuge tubes. The cultures centrifuged in a Beckman Avanti J-25 centrifuge at 9,500 rpm at 4 ^{o}C for 30 minutes using a JLA 10 Beckman rotor. The supernatant was discarded, and the pellet was resuspended and homogenized in 100 mL of pH 7.4, 50 mM phosphate equilibration buffer containing 15% glycerol. Cell walls were lysed with lysozyme for 30 minutes at room temperature while stirring. The lysed cells were then transferred to 25 mL centrifuge tubes and the membranes were degraded by sonication

using a Fisher Scientific 60 Sonic Dismembrator in four 30-second bursts at a power of 13W while on ice. The 25 mL centrifuge tubes were then transferred to a JA-20 Beckman rotor and centrifuged at 19,000 rpm for 30 minutes at 4 ^{o}C. Supernatant containing the CYP102A2 was decanted and saved. The cell fragments were discarded. CYP102A2 concentration was determined by UV-Vis spectrophotometry of the CO-reduced vs reduced heme.

Next, the crude CYP102A2 was applied to a purification column containing Whatman pre-swollen DE52 diethylaminoethyl cellulose anion exchange that had been equilibrated previously using about 5 column volumes of 50 mM phosphate buffer at pH 7.5 containing 15% glycerol. The extract was passed through the purification column in a chromatography refrigerator at 4 ^{o}C, and CYP102A2 remained on the column. The protein was eluted using an increasing concentration gradient of 50mM to 200mM NaCl in equilibration buffer. Flow through was collected in five 50 mL fractions and were tested for the presence of CYP102A2 using UV-Vis spectroscopy of the CO-reduced vs reduced heme of CYP102A2.

Fractions containing CYP102A2 were diluted with equilibration buffer to lower the NaCl concentrations in each to less than 20 mM. These dilutions were run through a fast flow Q-sepharose (GE Healthcare) column to apply the CYP102A2. This column had been pre-equilibrated with about 5 column volumes of 50 mM phosphate buffer at pH 7.5 containing 15% glycerol. Protein was eluted using an increasing concentration gradient of phosphate buffer from 100 to 300 mM at pH 7.4 with 15% glycerol. Flow through was collected in five 50 mL fractions. Fractions collected from the Q-sepharose column were

tested by spectrophotometry without further treatment using a Varian CARY 100 Bio UV-Visible Spectrophotometer. A quartz cuvette was filled with deionized water and a baseline was recorded from 250 nm to 500 nm. The water filled cuvette was then moved to the reference cell compartment, and a second quartz cuvette was used in the sample cell compartment to test the protein fractions collected from the size exclusion column. The samples were scanned from 250 nm to 500 nm in baseline subtraction mode. Fractions that displayed an absorbance ratio of 2:1, at 280 nm and 418 nm respectively were saved.

The pure fractions were diluted with 15% glycerol to lower the phosphate concentration to no more than 50 mM in each fraction. The dilutions were run through a short column of Whatman pre-swollen DE52 diethylaminoethyl cellulose anion exchange that had been equilibrated with pH 7.4 equilibration buffer. The applied CYP102A2 was eluted all at once as a tight, red band using 250 mM phosphate buffer at pH 7.4 and 100 mM NaCl with 15% glycerol. The purified protein was tested for CYP102A2 concentration using UV-Vis spectrophotometry of the CO-reduced heme of CYP102A2. The purified samples were then frozen at -80 ^{o}C.

II.T. CYP102A2 assay via UV-Vis spectrophotometry of the CO-reduced heme

The concentration of CYP102A2 in Hu227 cells was found using a variation of the method described by Omura and Sato [22] for detection of the hemoprotein, cytochrome P450. The extinction coefficient was assumed to be ε_{450}= 91 mM^{-1} cm^{-1}, and the concentration of CYP102A2 was determined from the spectra of the reduced CO vs reduced heme complexes.[17]

The CYP102A2 concentration in intact cells was determined by centrifuging a 2 mL aliquot of cultured cells from the Fernbach flask in a Fisher Scientific Centrific Centrifuge spinning at full speed for 10 minutes at 4 ^{o}C. The growth broth was discarded by decanting, and the cell pellet was resuspended in 2 mL of 50 mM phosphate buffer at pH 7.4 containing 15% glycerol. Next, 5 mg of sodium dithionite (Sigma) was dissolved in the 2 ml cell suspension to reduce the prosthetic heme iron of CYP102A2. One quartz cuvette was filled with 1 ml of the reduced cells and placed in the sample compartment of a Varian CARY 100 Bio UV-Visible Spectrophotometer. A baseline spectrum was recorded on the cells from 400 nm to 500 nm, and this cuvette was placed into the reference compartment of the spectrophotometer. A second cuvette was filled with the remaining 1 mL of reduced cells, and carbon monoxide gas was gently bubbled through the cell suspension for one minute to form the reduced CO complex. This cuvette was placed in the sample compartment, and the absorbance spectrum of the reduced vs reduced CO complex of CYP102A2 was recorded from 400 nm to 500 nm with the baseline subtracted. The reduced CO complex of CYP102A2 absorbed at 450 nm.

The CYP102A2 concentration in crude, cell-free extract was determined by diluting a 200 µL aliquot of the extract up to 2 mL with 50 mM phosphate buffer at pH 7.4 containing 15% glycerol. These 2 mL were divided between 2 quartz cuvettes. Next, a few grains of sodium dithionite were added, and a baseline spectrum was taken on 1 ml of the sample from 400 nm to 500 nm. Afterwards, that sample was moved to the reference compartment of the spectrophotometer. The remaining 1 ml of cells was gently bubbled with carbon monoxide for 1 minute, and a few grains of sodium dithionite were

added to form the reduced CO complex. This cuvette was placed in the sample compartment of the spectrophotometer, and the spectrum of the reduced vs reduced CO complex was taken with baseline subtraction. The procedure for finding the concentration of CYP102A2 in concentrated, purified samples was identical to that of the crude extract except that a 20 μL aliquot of purified sample was diluted up to 2 mL in this assay.

II.U. Activity assay of CYP102A2 with 12-*p*-nitrophenoxycarboxylic acid

The activity of the purified CYP102A2 was tested for 12-*p*-nitrophenoxycarboxylic acid (pNCA) as substrate by monitoring formation of the product *p*-nitrophenolate at 410 nm. The procedure was modified from that of Schwaneberg et al.[18] A quartz cuvette was filled with 7.5 μL of 6 mM pNCA in DMSO. Next, 0.1 nmol of CYP102A2 was added to the cuvette, and enough 0.1M Tris-HCl buffer at pH 8.2 was added to bring the solution up to a final volume of 1 mL. The cuvette was placed into the sample cell of a Varian CARY 100 Bio UV-Visible Spectrophotometer, and the blank spectrum was taken to zero the instrument. Next, 100 μL of 1mM NADPH was added to initiate the reaction. The absorbance at 410 nm was recorded every 2 seconds until there was no longer a change absorbance. A negative control spectrum was also taken for 200 seconds, where the reaction was never initiated by the addition of NADPH.

CHAPTER III

RESULTS AND DISCUSSION

III.A. Synthesis of ^{13}C and ^{15}N δ-aminolevulinic acid (ALA) isotopomers

The procedure for synthesizing the three isotopomers of aminolevulinic acid (ALA) that we selected was that of Wang and Scott[10]. This allowed for the production of [4-^{13}C] ALA, [5-^{13}C] ALA, and [^{15}N] ALA in a straight forward manner using four separate chemical steps. The synthesis of the phthalimidolevulinic acid ethyl ester was the key step in the procedure and required an extra amount of care to insure that any moisture was eliminated from the reaction. The overall yield for the most productive workup of ALA conducted was 67%, and the reported yield from the literature was 90%. Prior to working with the isotopically labeled derivatives of glycine, the total synthesis was performed starting from unlabeled glycine. This was done in order to refine the synthetic techniques without wasting large amounts of the much more expensive isotopomers of glycine. The amount of starting material was experimented with as well, where starting masses of glycine were either 0.5 g (6.7 mmol) or 1.0 g (13.3 mmol). Both starting masses were successfully worked up to the final product ALA, but the larger amount of starting material provided the most efficient synthesis.

Figure III.1. Synthesis of phthalylglycine from phthalic anhydride and glycine, with the numbering scheme shown.

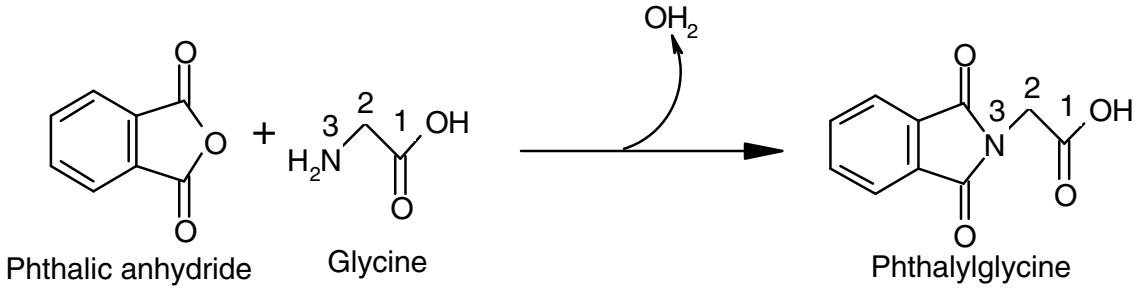

The formation of phthalylglycine was the first step in the synthesis, and the yield was near 90% in all attempts. This was relatively close to the reported yield of 98% from the literature. [1-^{13}C] glycine was used in the synthesis of [1-^{13}C] phthalylglycine, [2-^{13}C] glycine was used in the synthesis of [2-^{13}C] phthalylglycine, and [^{15}N] glycine was used in the synthesis of [^{15}N] phthalylglycine. Characterization of the products in each synthesis was achieved with ^{1}H-NMR spectroscopy. NMR data are displayed in Table III.1, and compared to the given literature values and chemical shift assignments. The ^{1}H-NMR experimental chemical shift and coupling constant values for [1-^{13}C] phthalylglycine were in agreement with the available reference values.[10]

The assigned chemical shifts of [2-^{13}C] phthalylglycine and [^{15}N] phthalylglycine were identical to those of [1-^{13}C] phthalylglycine. This was expected because the ^{13}C and ^{15}N isotopes should not affect the distribution of electrons in the molecules. Additionally, the large J coupling constant value observed in the [2-^{13}C] phthalylglycine ^{1}H-NMR data was indicative of hydrogens being split directly by a ^{13}C through a single bond. This degree of splitting strongly suggested, that there was a ^{13}C isotope incorporated at position two in phthalylglycine (Figure III.1)

[^{15}N] phthalylglycine sample displayed no splitting patterns in the ^{1}H-NMR spectrum with respect to the two hydrogens located at carbon 2 of the phthalylglycine structure. However, this reaction does not lend itself to the loss or replacement of a nitrogen atom, and it can be assumed that the ^{15}N was incorporated into the product. The [^{15}N] phthalylglycine sample shared identical chemical shifts with those of [1-^{13}C] phthalylglycine. These similar chemical shifts suggest that the connectivity of the ^{15}N labeled product is consistent with phthalylglycine.

Table III.1. ^{1}H-NMR data for the synthesized isotopomers of phthalylglycine, the available literature values, and chemical shift assignments.

	Experimental (^{1}H-NMR, ppm); (J, Hz)	Literature[10]	Assignment
[1-^{13}C] phthalylglycine	2.47 4.28 (^{2}J = 5.7) 7.88	 4.40 (J = 5.4) 7.82	m, DMSO (solvent) d, 2H, $CH_2{}^{13}CO$ AA'BB', 4H, H-Ph
[2-^{13}C] phthalylglycine	2.47 4.28 (^{1}J = 141.8) 7.88		m, DMSO (solvent) d, 2H, $^{13}CH_2CO$ AA'BB', 4H, H-Ph
[^{15}N] phthalylglycine	2.47 4.28 7.88		m, DMSO (solvent) d, 2H, $^{15}NCH_2CO$ AA'BB', 4H, H-Ph

Figure III.2. Synthesis of phthalimidoacetyl chloride from phthalylglycine and thionyl chloride, with the numbering scheme shown.

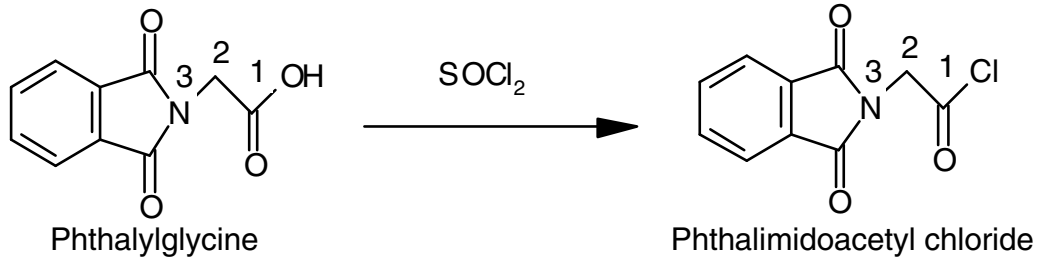

Phthalylglycine Phthalimidoacetyl chloride

The second step in the synthesis of ALA was the preparation of the phthalimidoacetyl chloride isotopomers. Extra care was taken to ensure that the reactant phthalylglycine was completely dry. Any moisture in the reaction with thionyl chloride would convert the acid chloride back to a carboxylic acid. Product yields of phthalimidoacetyl chloride isotopomers were near 98% in most attempts. Experimental ^{1}H-NMR data are compared to the available reference values, with the corresponding chemical shift assignments in Table III.2. The experimental chemical shift and J coupling constant values of [1-^{13}C] phthalimidoacetyl chloride were in good agreement with the literature values.[10] The chemical shifts of synthesized [2-^{13}C] phthalimidoacetyl chloride and [^{15}N] phthalimidoacetyl chloride were identical to those of [1-^{13}C] phthalimidoacetyl chloride. This suggested that each of the isotopomers possessed the desired connectivity corresponding to phthalimidoacetyl chloride.

The large J coupling constant associated with the chemical shift of 4.82 ppm in the data of [2-^{13}C] phthalimidoacetyl chloride suggested the presence of a ^{13}C atom incorporated into the two position of the phthalimidoacetyl chloride structure seen in Figure III.3. In this position, the attached hydrogens were split directly by ^{13}C through a single bond.

The chemical shifts corresponding to the hydrogens located at the two position were not split in the [^{15}N] phthalimidoacetyl chloride ^{1}H-NMR data. However, the presence of the chemical shift at 7.85 ppm demonstrated the conservation of the protecting group in the preceding reaction, and therefore the protected ^{15}N atom must have also been retained.

Table III.2. ^{1}H-NMR data for the synthesized isotopomers of phthalimidoacetyl chloride, the available literature values, and chemical shift assignments.

	Experimental (^{1}H-NMR, ppm); (J, Hz)	Literature[10]	Assignment
[1-^{13}C] phthalimidoacetyl chloride	4.82 (^{2}J = 5.8) 7.25 7.85	4.80 (^{2}J = 5.8) 7.78	d, 2H, $CH_2{}^{13}CO$ s, $CDCl_3$ (solvent) AA'BB', 4H, H-Ph
[2-^{13}C] phthalimidoacetyl chloride	4.82 (^{1}J = 146.3) 7.25 7.85		d, 2H, $^{13}CH_2CO$ s, $CDCl_3$ (solvent) AA'BB', 4H, H-Ph
[^{15}N] phthalimidoacetyl chloride	4.82 7.26 7.85		s, 2H, $^{15}NCH_2CO$ s, $CDCl_3$ (solvent) AA'BB', 4H, H-Ph

Figure III.3. Synthesis of phthalimidolevulinic acid ethyl ester from the coupling reaction of phthalimidoacetyl chloride and zinc homoenolate, with the numbering scheme shown.

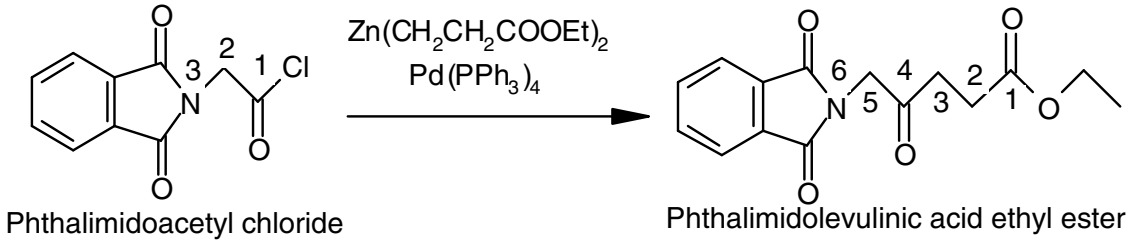

The third synthetic step was the key step in the synthesis of ALA.[10] This was the most labor intensive of the four steps in the synthesis. It was also imperative that reagents involved with this step were kept dry at all times as this was required for the formation of the zinc homoenolate. This step usually proceeded without incident, but in the cases where NMR data showed that products were not formed it was difficult to determine what had gone wrong. We soon learned to take every precaution possible to ensure that reagents were dry and always reacting under nitrogen gas.

The yield of phthalimidolevulinic acid ethyl ester from phthalimidoacetyl chloride was 90% in the most efficient synthesis conducted. This relatively high yield was in agreement with literature values for acylation reactions of homoenolate in the presence of a palladium catalyst (93%). ^{1}H-NMR data from the [4-^{13}C]-phthalimidolevulinic acid ethyl ester were in close agreement with the literature values. The spectral data are shown in Table III.3.

Chemical shifts in all of the isotopomers synthesized in this step were very similar, suggesting a connectivity that is consistent with phthalimidolevulinic acid ethyl ester. The ^{1}H-NMR data of the [5-^{13}C] phthalimidolevulinic acid ethyl ester showed splitting, with a large J coupling constant of 193.3 Hz, that was centered at the chemical shift 4.55 ppm. This chemical shift corresponded to the two hydrogens on the carbon five position. This large J value suggested that ^{13}C was present at the five position of the molecule, and that it was splitting the hydrogens directly connected through a single bond. No splitting was observed with respect to the hydrogens at the five position in [^{15}N] phthalimidolevulinic acid ethyl ester. The presence of the protecting group was evident however, as was shown by the multiplet at 7.80 ppm, and its presence suggested that the ^{15}N atom had been retained.

A key structural aspect of the phthalimidolevulinic acid ethyl ester was observed in the ^{1}H-NMR data of all of the isotopomers. The five protons of the ethyl ester group displayed chemical shifts at roughly 1.25 ppm as a triplet and 4.14 ppm as a quartet. The four protons on carbons two and three were also evident in all of the isotopomers. The chemical shift of the protons on carbon three was observed as a quartet between 2.74 and

2.85 in all of the isotopomers except for [4-^{13}C] phthalimidolevulinic acid ethyl ester. Here the peak was further split into a multiplet by the neighboring ^{13}C atom. The protons of carbon two were also split into a multiplet by the nearby ^{13}C atom of [4-^{13}C] phthalimidolevulinic acid ethyl ester and were centered at 2.65 ppm. These protons were also seen at the same chemical shift in the ^{1}H-NMR of the other two isotopomers, but they existed as triplets due to the lack of another nearby atom with a nuclear spin I = ½.

Table III.3. ^{1}H-NMR data for the synthesized isotopomers of phthalimidolevulinic acid ethyl ester, the available literature values, and chemical shift assignments.

	Experimental (^{1}H-NMR, ppm); (J, Hz)	Literature [10]	Assignment
[4-^{13}C] phthalimidolevulinic acid ethyl ester	1.24 (^{3}J = 7.2) 2.65 2.74 4.13 (^{3}J = 7.2) 4.55 (^{2}J = 4.0) 7.25 7.80	1.26 (^{3}J = 7.2) 2.65 2.84 4.14 (^{3}J = 7.2) 4.56 (^{2}J = 4.0) 7.80	t, 3H, $CH_2C\underline{H}_3$ m, 2H, $^{13}COCH_2C\underline{H}_2$ m, 2H, $^{13}COC\underline{H}_2CH_2$ q, 2H, $OC\underline{H}_2CH_3$ d, 2H, $NCH_2{}^{13}CO$ s, $CDCl_3$ (solvent) AA'BB', 4H, H-Ph
[5-^{13}C] phthalimidolevulinic acid ethyl ester	1.25 (^{3}J = 7.4) 2.65 (^{3}J = 6.7) 2.84 (^{3}J = 6.4) 4.14 (^{3}J = 7.3) 4.55 (^{1}J = 193.3) 7.25 7.80		t, 3H, $CH_2C\underline{H}_3$ t, 2H, $COCH_2C\underline{H}_2$ t, 2H, $COC\underline{H}_2CH_2$ q, 2H, $OC\underline{H}_2CH_3$ d, 2H, $N^{13}CH_2CO$ s, $CDCl_3$ (solvent) AA'BB', 4H, H-Ph
[^{15}N] phthalimidoacetyl chloride	1.25 (^{3}J = 7.4) 2.65 (^{3}J = 6.9) 2.85 (^{3}J = 6.9) 4.14 (^{3}J = 6.9) 4.55 7.25 7.80		t, 3H, $CH_2C\underline{H}_3$ t, 2H, $COCH_2C\underline{H}_2$ t, 2H, $COC\underline{H}_2CH_2$ q, 2H, $OC\underline{H}_2CH_3$ s, s, 2H, $^{15}NCH_2CO$ $CDCl_3$ (solvent) AA'BB', 4H, H-Ph

Figure III.4. Synthesis of aminolevulinic acid from the acid hydrolysis of phthalimidolevulinic acid ethyl ester, with the numbering scheme shown.

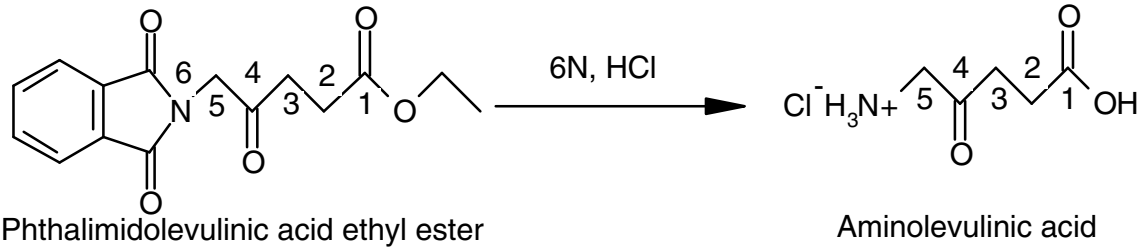

Phthalimidolevulinic acid ethyl ester

Aminolevulinic acid

The final reaction in the synthesis of aminolevulinic acid (ALA) was the acid hydrolysis and deprotection of the phthalimidolevulinic acid ethyl ester. Product yield was close to 90% in most attempts. The yield for the overall synthesis was 67% in the most efficient synthesis conducted. This was accomplished by beginning with 1.01 grams (13.28 mmol) of the starting material glycine, yielding 1.51 grams (8.92 mmol) of aminolevulinic acid after the completion of the four synthetic steps. Recrystalization of the ALA from ethanol and ether provided sufficiently pure product for the growth of *E. coli* HU227. This was also a cost effective method of obtaining the ALA isotopomers.

^{1}H-NMR data for [4-^{13}C] ALA and [^{15}N] ALA agreed well with the literature values, and all data are shown in Table III.4. The chemical shifts in all experimental ^{1}H-NMR are slightly lower than the literature values that were available by about 0.2 ppm in each case, but these small upfield shifts are observed in all of the chemical shifts. This may be due to a bad reference lock in the solvent D_2O, as the solvent used for each NMR sample came from the same source. Despite this small discrepancy, the J coupling constants are very similar to the literature values in general, and are indicative of the structure of aminolevulinic acid.

The peak of the chemical shift at 2.76 ppm in the [4-^{13}C] ALA sample, which corresponds to the protons of carbon three, was split into a distinct multiplet. This suggests that the incorporation of a ^{13}C label in the four position of ALA has been accomplished. If there were no ^{13}C nearby this position, as in the [^{15}N] ALA sample, the protons of carbon three would only be expected to split into a triplet. This is indeed what is seen in the [^{15}N] ALA sample at 2.73 ppm. Interestingly, the [5-^{13}C] ALA sample showed a much less distinct multiplet character. This indicated that the ^{13}C atom at the five position of [5-^{13}C] ALA was splitting the protons at the three position to a minor extent. A similar effect was seen in the chemical shift at 2.55 ppm of [4-^{13}C] ALA, where the protons that were three bonds away were also split into a slight multiplet by the ^{13}C atom in the four position of the molecule. These particular protons, in position two of the molecule, were left unaffected by the ^{13}C atom of [5-^{13}C] ALA as it was too far away. In this case, these protons were merely split by their neighboring protons into a triplet. The same characteristic was seen in [^{15}N] ALA.

The chemical shift at 3.97 ppm of the [4-^{13}C] ALA sample suggested that the ^{13}C atom was in the four position, as it was able to significantly split its neighboring protons into a doublet with a J coupling constant of 4.2 Hz. These same protons were even more significantly split (J = 143.3) in the [5-^{13}C] ALA sample, which suggested that these protons were directly bonded with the ^{13}C atom. This provided significant evidence that a ^{13}C atom was incorporated at the five position of the molecule.

Finally, no chemical shifts were split due to the ^{15}N atom in the [^{15}N] ALA sample. Even though this left us without a method of positively identifying the presence

of a ^{15}N atom in the molecule, we were reasonably sure of its presence. The high level of purity in the synthetic starting material [^{15}N] glycine, and the fact that none of the reactions carried out in the synthesis lended themselves to the loss of a nitrogen atom was enough to assure us that the ^{15}N atom was incorporated. Additionally, the group that originally devised this method of ALA synthesis reported that they successfully generated [^{15}N] ALA using this method. Furthermore, our [^{15}N] ALA ^{1}H-NMR data matched well with what had been reported previously.[10, 28]

Table III.4. ^{1}H-NMR data for the synthesized isotopomers of aminolevulinic acid, the available literature values, and chemical shift assignments.

	Experimental (^{1}H-NMR, ppm); (J, Hz)	Literature [10, 28]	Assignment
[4-^{13}C] aminolevulinic acid	2.55 2.76 3.97 (^{2}J = 4.2)	2.71 2.90 4.13 (^{2}J = 3.9)	m, 2H, $^{13}COCH_2C\underline{H}_2$ m, 2H, $^{13}CO\underline{CH}_2CH_2$ d, 2H, $NCH_2{}^{13}CO$
[5-^{13}C] aminolevulinic acid	2.53 (^{3}J = 6.2) 2.73 3.95 (^{1}J = 143.3)		t, 2H, $COCH_2C\underline{H}_2$ m, 2H, $CO\underline{CH}_2CH_2$ d, 2H, $N^{13}CH_2CO$
[^{15}N] aminolevulinic acid	2.52 (^{2}J = 6.9) 2.71 (^{2}J = 6.1) 3.95	2.60 (^{2}J = 6.3) 2.78 (^{2}J = 6.3) 4.01	t, 2H, $COCH_2C\underline{H}_2$ t, 2H, $CO\underline{CH}_2CH_2$ s, 2H, $^{15}NCH_2CO$

The method for the synthesis of isotopomers of aminolevulinic acid, developed by Wang and Scott[10], was relatively simple and cost effective for our purposes. However, we were not able to achieve the high overall yield of 90% that they originally reported. Monitoring the formation of our product with ^{1}H-NMR also seemed to be logical and productive. That is because changes in the chemical shifts, going from reactants to

products in each synthetic step, were significant enough to make ^{1}H-NMR a valuable tool for the characterization of our isotopomers.

III.B. Expression and purification of dehaloperoxidase

For reasons discussed previously, dehaloperoxidase (DHP) was chosen as a representative heme protein for ^{13}C and ^{15}N incorporation. Our expression system consisted of a DHP encoding plasmid transformed into the *E. coli* Hu227 cells, where gene expression was under the control of a *lac* promoter. The synthesized isotopomers of aminolevulinic acid (ALA) were required for the cells to survive as they were incapable of generating the ALA on their own. This ensured the incorporation of ^{13}C and ^{15}N labels as the cells synthesized the heme for DHP because their only supply of the heme precursor was the isotopomer of ALA in the growth media.

DHP was successfully overexpressed and purified from *E. coli* HU227 cells grown in Luria Bertani growth media containing the synthesized isotopomers of aminolevulinic acid. A typical absolute absorbance spectrum of the CO-reduced heme complex of purified DHP is displayed in Figure III.5. It can be seen that the λ-max was approximately 423 nm. Spectra of the CO-reduced heme complex of DHP in the whole cells displayed a λ-max at 420 nm with an absorption of about 0.030 in cultures displaying good expression. Typical yields of DHP were moderate after purification, and were between 91.5 and 189 nmoles of protein per liter of growth media.

Figure III.5. Absolute absorbance spectrum of the CO-reduced heme complex of purified dehaloperoxidase.

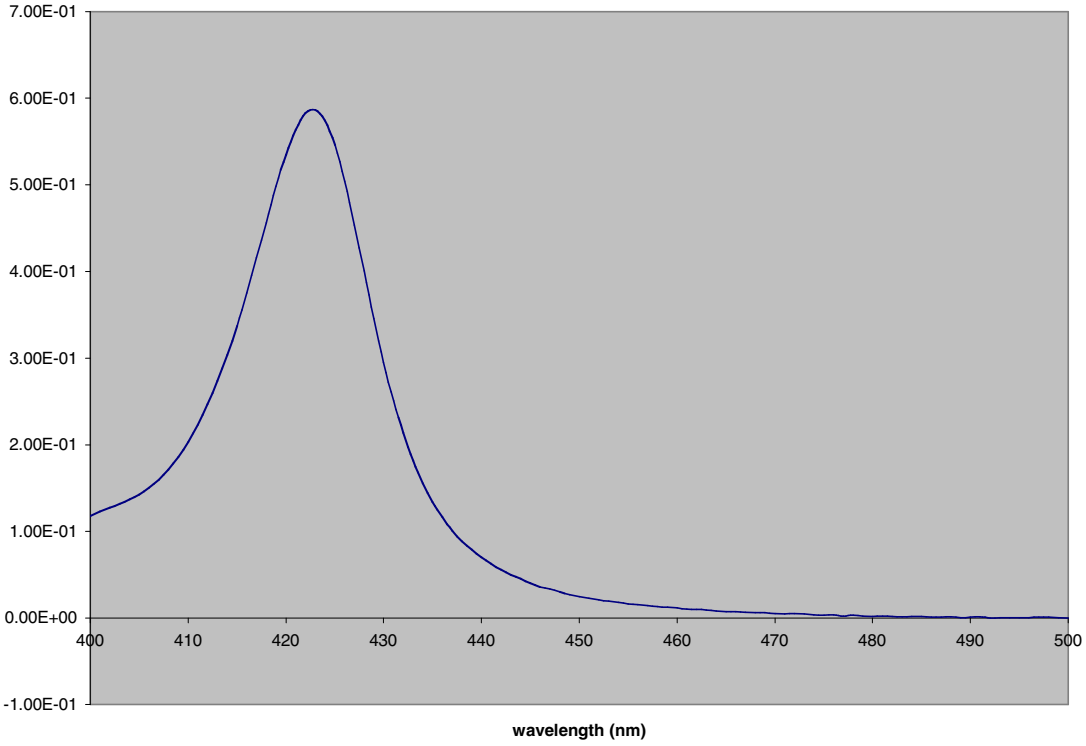

III.C. MALDI-TOF and LC-MS analysis of isotopically labeled heme from dehaloperoxidase

Matrix-assisted laser desorption/ionization-time of flight mass spectrometry (MALDI-TOF) was conducted on heme isotopomers that had been extracted and purified from dehaloperoxidase. Unlabeled heme from DHP that was overexpressed with unlabeled aminolevulinic acid (ALA), and labeled heme from DHP that was overexpressed with [5-^{13}C] ALA are shown in Figures III.6 and III.7 respectively. Neither the [4-^{13}C] ALA or [^{15}N] ALA gave MALDI-TOF spectra that could be

interpreted. It is likely that the samples were either too impure, or had degraded prior to analysis.

When comparing the MALDI-TOF spectrum of the unlabeled heme sample (Figure III.6) to the labeled heme sample (Figure III.7), an increase of 8 amu was observed in the major peak of interest. The mass increase from 616 m/Z to 624 m/Z suggests that eight ^{13}C atoms were successfully incorporated into the heme biosynthetically, as was predicted. Presently, we have not been able to characterize the second major peak in each of the MALDI-TOF figures. If these peaks were due to a heme dimer complex of some kind, a coordinating molecule would need to present to stabilize the structure. However, the difference in m/Z between the major peaks in Figure III.6 is not equal to the difference in m/Z between the two peaks in Figure III.7. This eliminates the possibility of a single type of molecule coordinating such a heme complex in both of the MALDI-TOF spectra. It is more likely that these secondary peaks are due to contamination or impurities of the heme samples, given that these samples were not purified extensively.

Figure III.6. MALDI-TOF spectrum of unlabeled heme from DHP, displaying a major peak at *m*/Z value of 616.

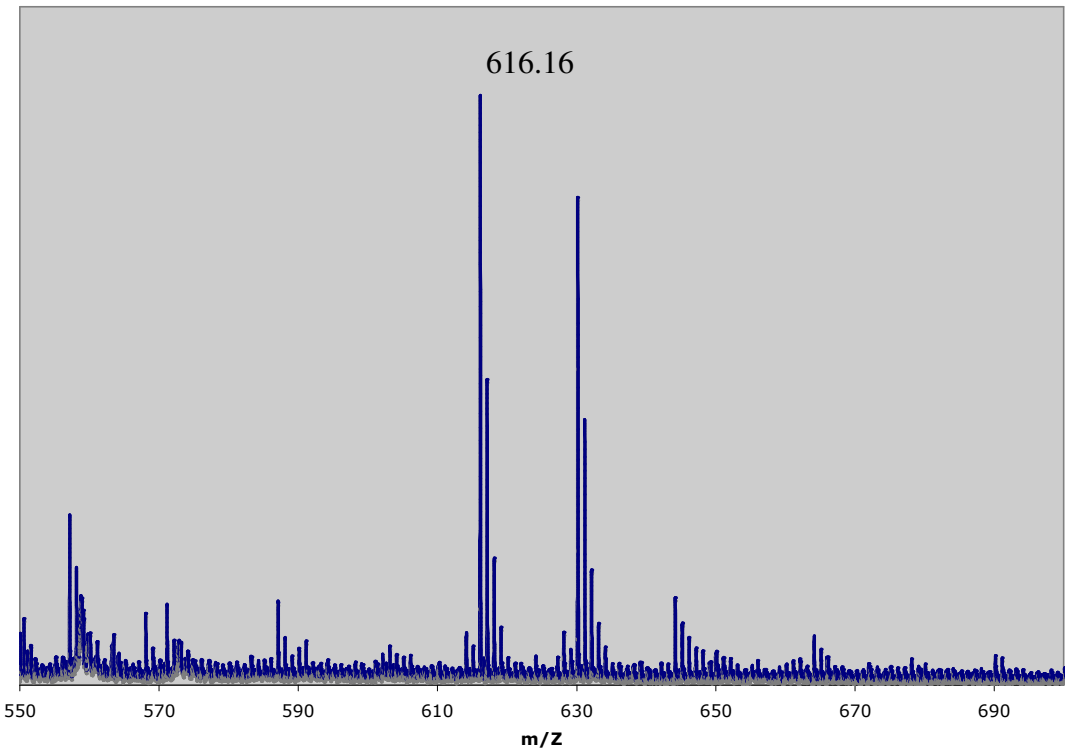

Figure III.7. MALDI spectrum of ^{13}C labeled heme from DHP grown in [5-^{13}C] ALA, displaying a major peak at *m*/Z value of 624.

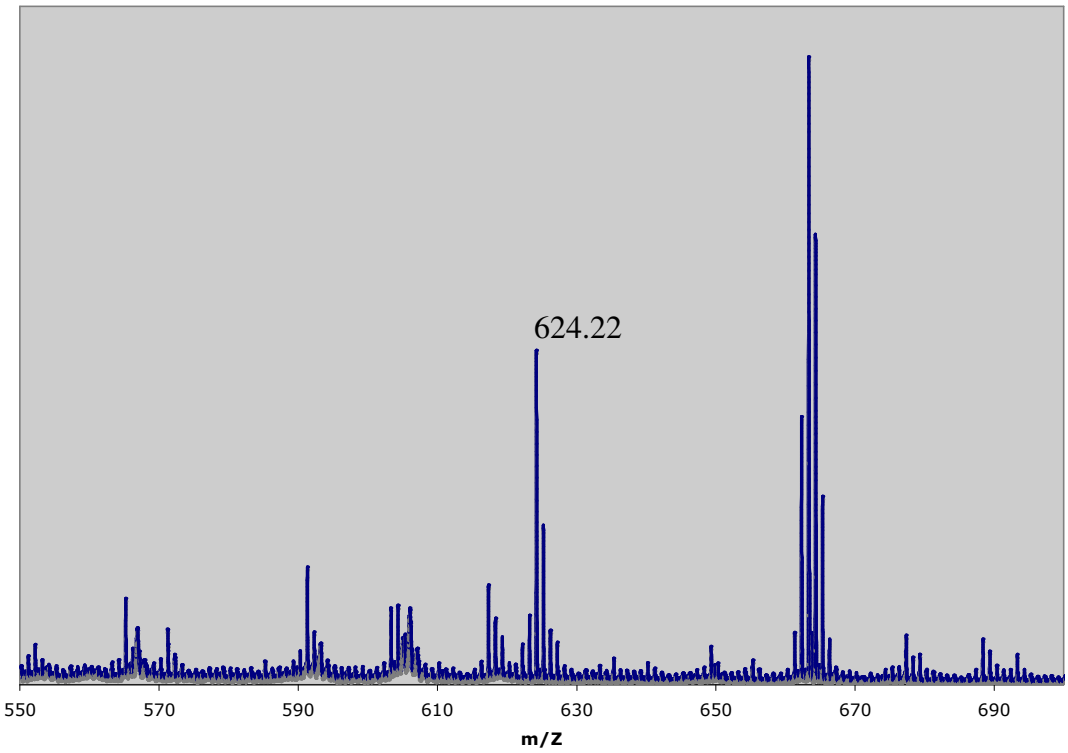

After the failure to generate significantly pure MALDI-TOF samples of the biosynthetically labeled heme, we decided to try a different approach. Other researchers have shown that it is possible to separate and identify the mass of *tert*-butyl 1-methyl-2-propynyl ether adducted hemes (705 Da) in a protein sample using high performance liquid chromatography-mass spectrometry with electrospray ionization (LC-MS).[29] Under similar conditions, attempts were made to analyze HPLC purified, isotopically labeled heme samples with LC-MS. The LC-MS chromatograms of the three isotopomers of heme are displayed in Figure III.8. All three samples displayed remarkably similar retention times and resolution. The labeled heme was eluted at about 29 minutes in each

run. It can also be seen in the chromatogram that there are large peaks flanking the 29 minute elution peak. Although we were not able to characterize the contents of these peaks, it is likely that these are protein fragments that were dissolved in the sample, and were not well separated from the heme in the reverse phase column of the HPLC prior to LC-MS analysis. The amount of impurities relative to the heme analyte provides some insight into the level of purity in the MALDI-TOF samples discussed earlier. In these samples, heme was merely purified in a short C18 sep-pak column, so the level of purity would have been greatly reduced. Upon realizing this, it is reasonable that some of our MALDI-TOF samples were not viable. The exact masses of each heme sample, corresponding to the heme elution times of the LC-MS chromatograms, are shown in Figures III.9, III.10, and III.11.

The masses of heme synthesized biosynthetically from [4-^{13}C] ALA and [5-^{13}C] ALA are shown in Figures III.9 and III.10 respectively. Both samples displayed a major peak at 624.2 m/Z. This is consistent with the expected mass for these isotopomers, and suggests that the incorporation of eight ^{13}C atoms into the prosthetic heme was successful as was indicated previously in the MALDI-TOF data for [5-^{13}C] ALA.

There are also two additional major peak in each of the three figures corresponding to the exact masses. These two major peaks are of identical mass in each sample, and therefore are not related to the heme itself. These peaks are probably representative of impurities in the samples, as they were each prepared in the sample manner.

The mass of heme synthesized biosynthetically from [^{15}N] ALA is shown in Figure III.11. The major peak at 620.2 m/Z is also consistent with the expected mass for this isotopomer, and suggests that four ^{15}N atoms were successfully incorporated into the heme. This is significant because the biosynthesis of ^{15}N labeled heme via this route has not been previously described.

Figure III.8. LC-MS chromatogram of purified isotopically labeled heme from DHP. (a.) Heme purified from DHP overexpressed in [4-^{13}C] ALA. (b.) Heme purified from DHP overexpressed in [5-^{13}C] ALA. (c.) Heme purified from DHP overexpressed in [^{15}N] ALA. (*) marks the peak corresponding to elution of heme.

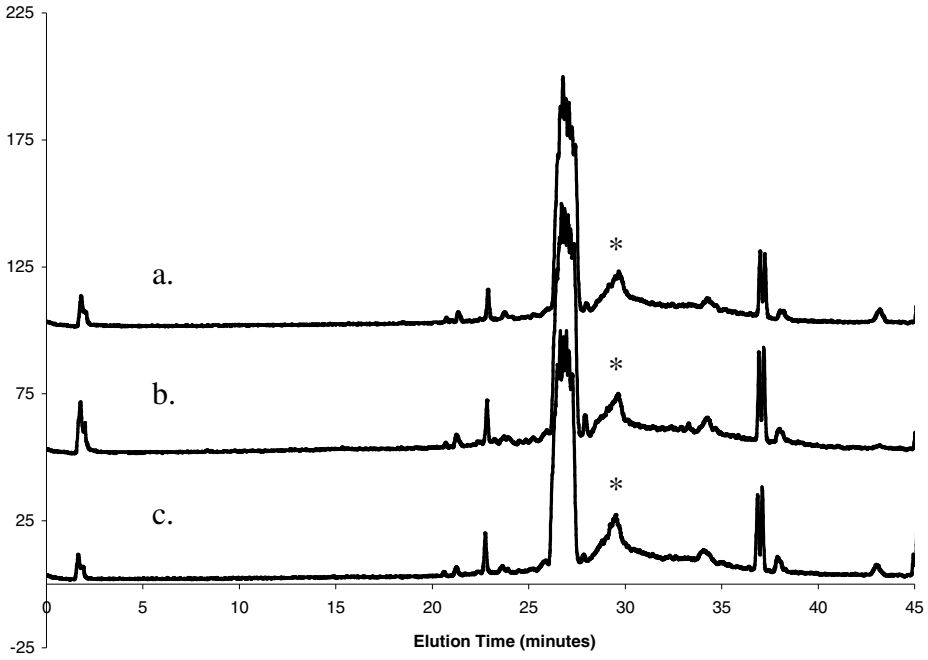

Figure III.9. Exact masses of components contained in the peak corresponding to the elution of heme in chromatogram (a) of Figure III.8 containing heme purified from DHP overexpressed in [4-^{13}C] ALA.

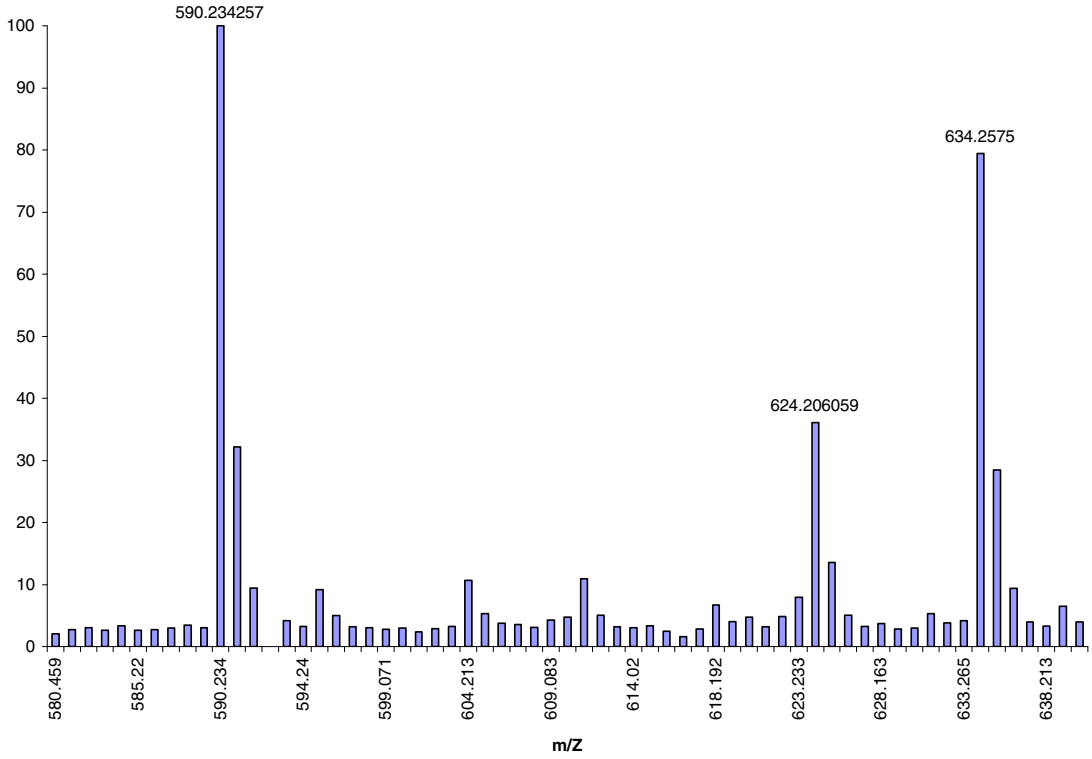

Figure III.10. Exact masses of components contained in the peak corresponding to the elution of heme in chromatogram (b) of Figure III.8 containing heme purified from DHP overexpressed in [5-^{13}C] ALA.

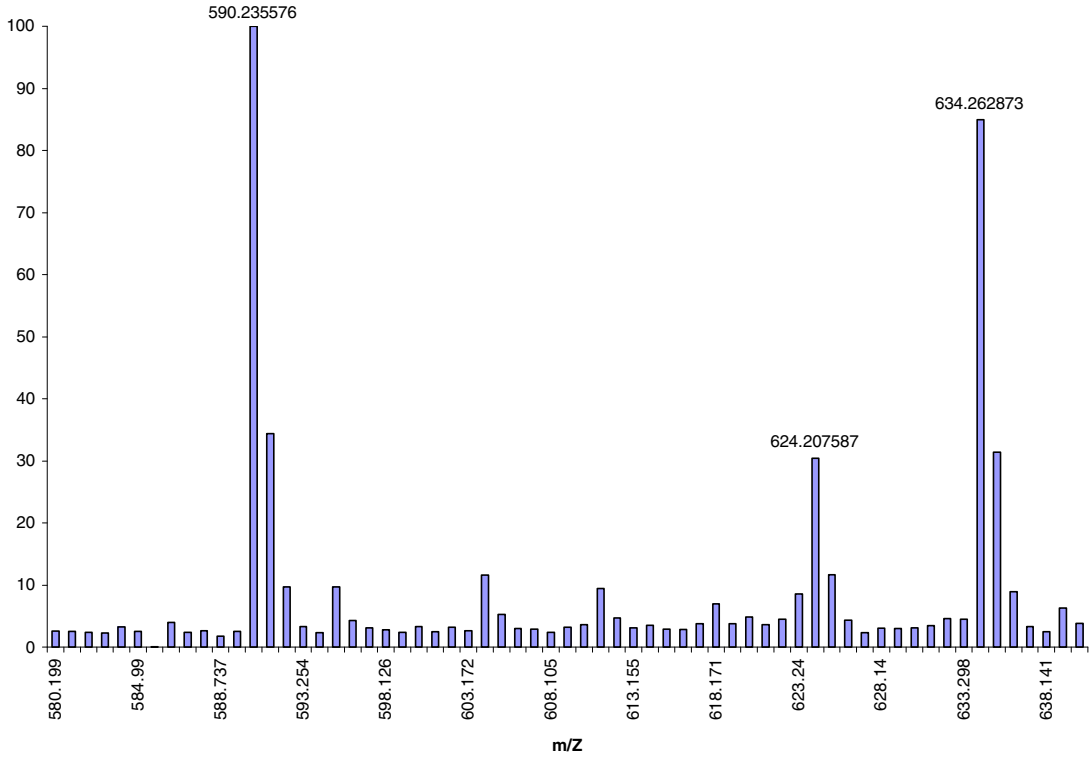

Figure III.11. Exact masses of components contained in the peak corresponding to the elution of heme in chromatogram (c) of Figure III.8 containing heme purified from DHP overexpressed in [^{15}N] ALA.

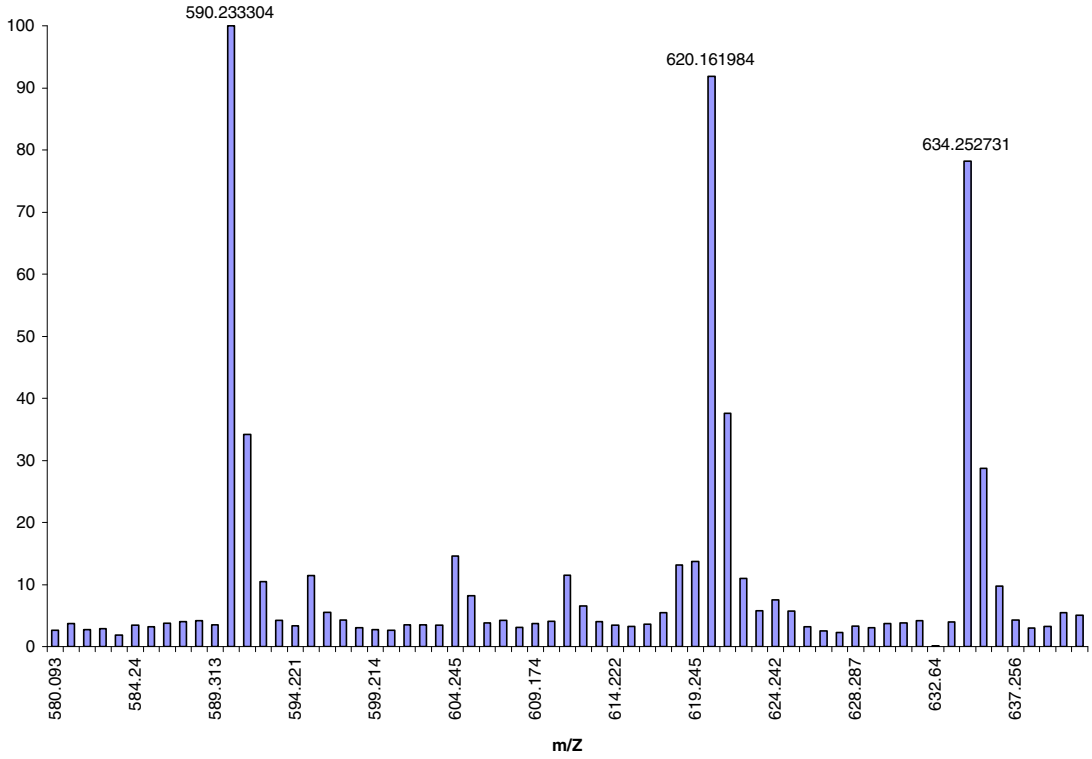

III.D. Cloning of the CYP102A2 gene of *Bacillus Subtilis 168*

One of the goals in this project was to generate a recombinant plasmid containing an expression vector and the CYP102A2 gene. The long-term goal of this project is to be able to use this recombinant plasmid in the ^{13}C- and ^{15}N-heme incorporating expression system. The current system for production of P450 BM3 in this lab involves a plasmid containing a T7 promoter for control of expression.[30, 31] *E. coli* Hu227 cells do not contain the gene that expresses the T7 polymerase, so these plasmids would not be expressed in Hu227 cells without first transfecting the cells with the DNA that would allow T7 polymerase expression.

Our first attempt at solving this expression problem was to utilize a two-plasmid system. The goal was to transform the Hu227cells with a plasmid that encoded for the T7 polymerase and imparted kanamycin resistance, and then transform with a second plasmid that encoded for the P450. Problems arose with this system because of the difficulty in transforming Hu227. This strain of cells is difficult to make competent in order to perform the transformations. Furthermore, once both plasmids were finally transformed into the cells, no expression was ever observed after induction with IPTG. This 2-plasmid expression system was soon abandoned after generating the transfected cells.

We have been able to generate a recombinant plasmid containing an expression vector under the control of a *lac* promoter, and the CYP102A2 gene. This was accomplished using a method modified from Gustafsson et al.[17] The first step was to amplify the CYP102A2 gene from genomic *Bacillus subtilis 168* DNA. A polymerase chain reaction (PCR) was used to accomplish this, and the PCR product was confirmed by agarose gel electrophoresis, shown in Figure III.12. It can be seen in lanes 1 and 2 containing the PCR product, that the size of the fragment is near 3183 base pairs, which is the size of the CYP102A2 gene according to the published sequence listed by the *Bacillus subtilis* data bank.

Figure III.12. 1% Agarose electrophoresis gel containing polymerase chain reaction products. Lanes 1 and 2 both contain PCR product containing CYP102A2 gene.

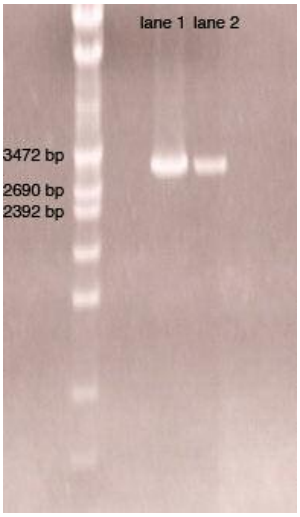

The next step was to cut both the expression vector and PCR product in order to generate complementary ends on each. This would allow the vector and PCR product to be ligated together in a subsequent step. The primers used in the PCR reaction in the previous step inserted two restriction sites, which flanked the CYP102A2 gene. An *Xba*I restriction site was cloned outside the 5' end of the CYP102A2 coding region, and an *Xho*I restriction site was cloned outside the 3' end of the coding region. These restriction sites in the PCR product were cut in this step, as were these same sites in the multicloning region of the pbluescript II SK(-) vector.

Controls were also conducted in the restriction digest steps in order to ensure that both restriction enzymes were functioning properly. The results of all restriction digests are seen in the agarose gel in Figure III.13. Lanes 1 and 2 of the gel show the cut PCR product and expression vector respectively. It is apparent that these two fragments are similar in size, which is predicted based on the expected size of the PCR product versus

the linear plasmid. Lanes 3 and 4 show the results of the control experiments where one restriction enzyme was omitted in each reaction. These controls showed that the restriction enzymes were both active. If one of the enzymes had not cut the vector substrate, the bands in lanes 3 and 4 would not both be similar in size to the cut vector in lane 2.

Figure III.13. 1% Agarose electrophoresis gel containing restriction digest products. Lane 1 contains digest of the CYP102A2 gene from the PCR. Lane 2 contains digest of pbluescript II SK(-) vector. Lane 3 contains digest of vector with restriction enzyme XhoI in the absence of XbaI. Lane 4 contains digest of vector with restriction enzyme XbaI in the absence of XhoI.

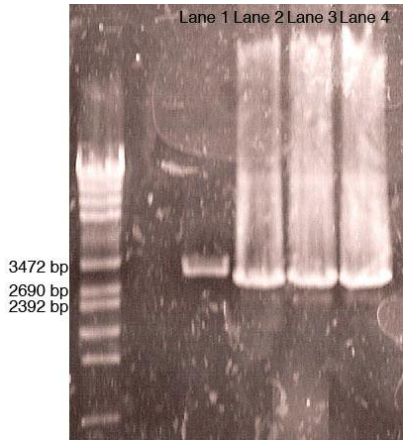

The cut PCR product and vector were then included in ligation reactions. However, the ligation products needed to be screened for the presence of both the CYP102A2 gene and the expression vector. This was accomplished in two screening procedures. In the first screen the ligation product was transformed into XL1-Blue cells, and they were grown on agar plates containing ampicillin. Any colonies that grew on the plates were known to at least contain the expression vector. This was because the expression vector is what provided the cells with ampicillin resistance. Individual

colonies of the transformed cells were grown overnight to produce large amounts of the plasmid, which were isolated from each culture the next day. The purified plasmids were passed through an agarose gel for analysis (Fig III.14), and any plasmids that were nearly twice the size of cut PCR product or cut expression vector were saved. These were the most likely candidates to contain the expression vector with the P450 gene incorporated. It can be seen that the plasmid in lane three of Figure III.14 was the most likely candidate out of the 7 plasmids shown in the gel, since it appears to be nearly twice the size of the native vector.

Figure III.14. 1% Agarose electrophoresis gel containing purified plasmids from XL1-Blue cells transformed with ligation products. Lane 1 contains undigested pbluescript II SK(-) vector. Lane 2 contains undigested CYP102A2 gene from PCR. Lanes 3 through 9 contain purified plasmids from individual colonies of transformed XL1-Blue cells.

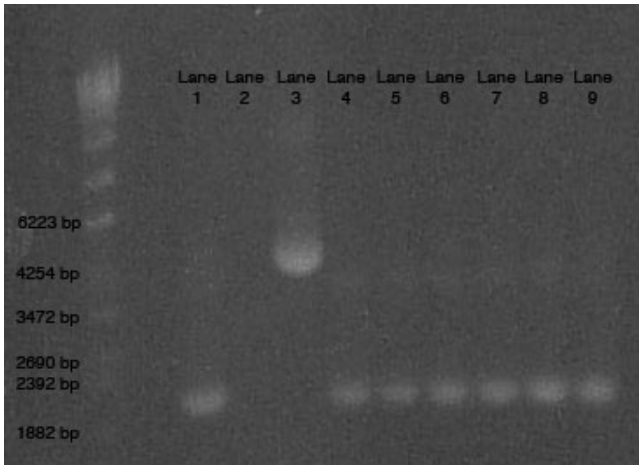

Good candidates from the first screening step were taken on to the second screen. This screen was accomplished by PCR, using the 102A21 and 102A22 primers on the individual purified plasmid samples. The PCR products were analyzed by 1% agarose gel electrophoresis (Fig III.15), and the band sizes were compared to cut CYP102A2-insert.

The band sizes that were close in size to the CYP102A2-insert suggested that the desired DNA fragment had been ligated into the pbluescript II SK(-) vector.

Figure III.15. 1% Agarose electrophoresis gel containing PCR products of purified plasmids from XL1-Blue cells transformed with ligation products. Lane 1 contains the negative control PCR product of non-recombinant pbluescript II SK(-) vector. Lane 2 contains undigested CYP102A2 gene from PCR. Lanes 3 through 9 contain PCR products of the purified plasmids from individual colonies of transformed XL1-Blue cells shown in Fig.5.

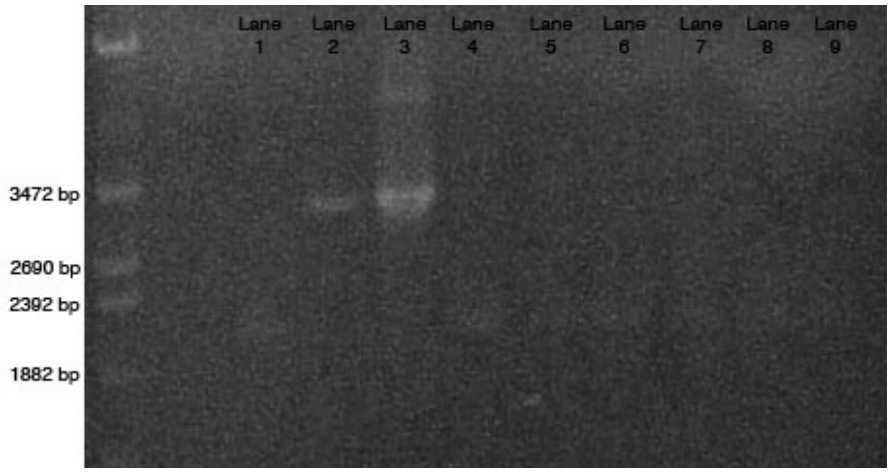

III.E. Expression and purification of CYP102A2

CYP102A2 was successfully overexpressed and purified from *E. coli* HU227 cells grown in Terrific Broth growth media containing the unlabeled aminolevulinic acid (ALA) (Acrōs). A typical absorbance spectrum of the reduced heme versus CO-reduced heme complex of CYP102A2 in whole cells is displayed in Figure III.16. The strong heme absorbance at 450 nm associated with P450 enzymes makes it possible to track expression of P450 enzymes in whole cells by difference spectrophotometry. This is very useful in determining whether to harvest cells based on their expression. Typical yields of CYP102A2 were much lower than those seen in dehaloperoxidase after purification, and

were about 4 nmoles of protein per liter of growth media. The purified CYP102A2 was passed through a sodium dodecyl sulfate-polyacrylamide gel shown in lane six of Figure III.17. Two bands were observed, where one band at about 119 kilodaltons was expected.[26] Our data suggest that there was some level of degradation in the sample. Despite the low yields displayed by CYP102A2, we have shown that it is possible to generate this protein in our expression system with unlabeled ALA; and therefore, it should be possible to isotopically label the prosthetic heme of CYP102A2 biosynthetically using isotopomers of ALA, particularly with improved purification strategies. However, more experiments should be conducted to optimize the growth conditions of the protein with unlabeled ALA, in order to make labeling experiments cost effective.

Figure III.16. Absorbance spectrum of reduced vs CO-reduced heme complex of CYP102A2 in whole cells.

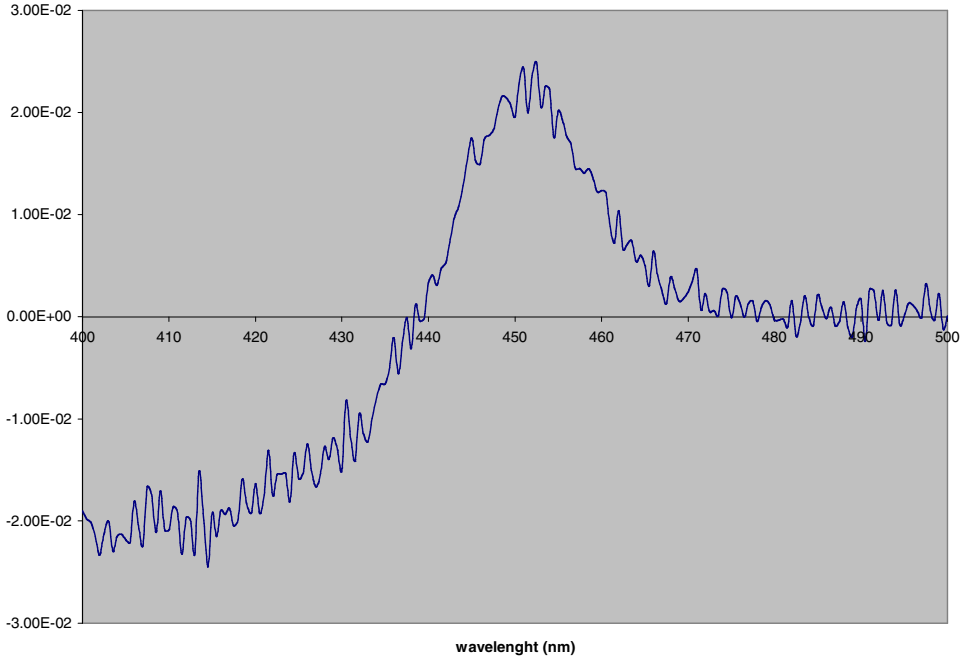

Figure III.17. SDS-PAGE gel; lane 1 = molecular weight marker, lane 2 = purified DHP grown with [4-^{13}C] ALA, lane 3 = purified DHP grown with [5-^{13}C] ALA, lane 4 = purified DHP grown with [^{15}N] ALA, lane 5 = purified DHP stock with unlabeled heme, lane 6 = purified CYP102A2.

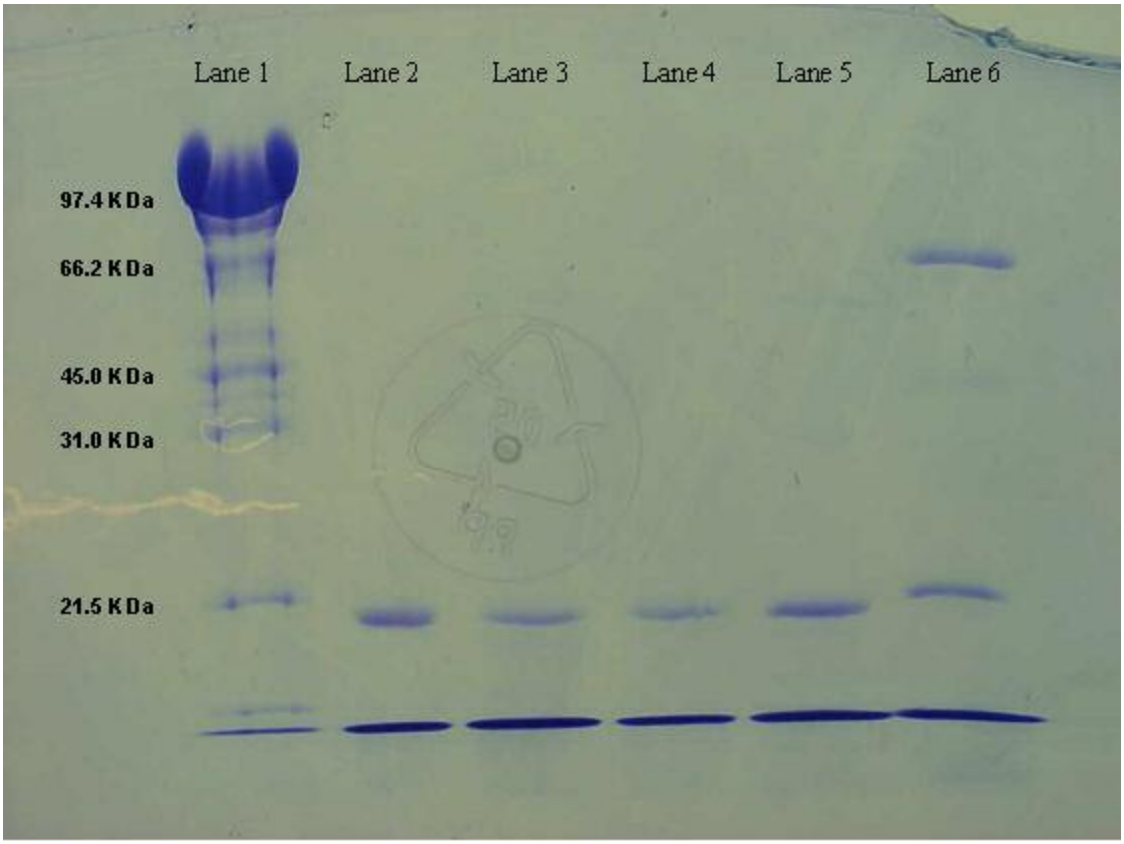

III.F. Activity assay of CYP102A2 with 12-*p*-nitrophenoxycarboxylic acid

The ability of purified CYP102A2 to catalyze the hydroxylation of 12-*p*-nitrophenoxycarboxylic acid (pNCA) and generate the product *p*-nitrophenolate was studied, and rates were compared to similar studies conducted with the P450 BM-3 and BM-3 F87A mutant. The rate of catalysis in CYP102A2 was much less than both reported values for the wild-type P450 BM-3 and the BM-3 F87A mutant. Control experiments, where the electron donor NADPH was not added, showed no enzymatic

activity over 200 seconds. Reduced activity compared to the P450 BM-3 and BM-3 F87A may suggest that the active site of CYP102A2 does not accommodate saturated, medium chain, unbranched fatty acids well. It should also be noted that, in another study[17], catalytic rates were generally higher in unsaturated and branched chain fatty acids. It is also possible that the reduced catalytic activity is due to protein degradation. The sodium dodecyl sulfate-polyacrylamide gel in Figure III.17 shows two bands in lane six, where a single band at around 119 kilodaltons was expected. Although further studies are needed, it appears that P450102A2 has a lower turnover rate than its relative BM3 in the oxidation of straight chain fatty acids.

Table III.5. Enzymatic activity of P450 isoforms CYP102A2 and BM-3 with pNCA

	CYP102A2	BM-3 wild-type[18]	BM-3 F87A[18]
Enzymatic activity over 200 seconds [k_{cat} = (nmol of product * nmol of $P450^{-1}$ * min^{-1})	4.24	114	508

CHAPTER IV

CONCLUSIONS

^{13}C NMR will be a powerful tool for probing the distribution of electrons in cytochrome P450 enzymes. We have developed a novel expression system that allows for high levels of ^{13}C and ^{15}N incorporation into the native heme of these enzymes. This will eliminate the need to reconstitute apo-proteins with labeled exogenous heme as has typically been done for other hemoproteins. *E. coli* Hu227 cells cannot synthesize their own aminolevulinic acid, which is a heme precursor in the biosynthesis of the porphyrin ring. This bacterial strain provided us with a way to selectively label the heme of any hemoprotein we chose to overexpress, provided that the gene expression vector was compatible with the Hu227 cells.

Cytochromes P450 have typically been expressed under the control of a T7 promoter in past studies. Such expression vectors are not compatible with Hu227 cells because they do not carry a T7 polymerase. We chose dehaloperoxidase as a heme containing model protein because it was under the control of a lac operon.

[4-^{13}C] aminolevulinic acid, [5-^{13}C] aminolevulinic acid, and [^{15}N] aminolevulinic acid were synthesized from the starting material glycine and characterized using ^{1}H-NMR with great success. These isotopomers were supplemented to *E. coli* Hu227 cells for the labels to be incorporated into the heme of dehaloperoxidase (DHP). Although we do not currently have the expertise to conduct the ^{13}C-NMR studies ourselves, we were successful in generating a highly concentrated (~1 mM) NMR sample of purified DHP.

This DHP sample had been overexpressed in growth media supplemented with [5-^{13}C] ALA. Samples of DHP that had been overexpressed with the other two isotopomers of ALA were also generated, but the stocks of these proteins were not large enough to generate viable NMR samples.

Additionally, the LC-MS data of HPLC purified heme samples displayed masses that were consistent with the incorporation of either eight ^{13}C labels or four ^{15}N labels, depending on which isotopomer of ALA was supplied to the cells during overexpression. These mass increases were precisely what were expected given that eight molecules of aminolevulinic acid were required for the biosynthesis of a single heme molecule, and that one nitrogen atom from each porphobilinogen (PBG) molecule was removed by PBG deaminase during the heme biosynthesis as well.

Finally, we successfully generated a recombinant expression vector that contained the CYP102A2 gene from *Bacillus subtillis* 168 that was under the control of a *lac* promoter. This expression vector was shown to be compatible with the Hu227 cells and displayed moderate expression in the whole cells (~ 200 nmol/ liter of culture). However, the purification techniques of this enzyme need to be refined before isotopic labeling of the heme can be done economically. The low activity of the enzyme that we observed may be due to degradation of the protein. Multiple bands were observed from the protein sample in the SDS-PAGE, and this suggests some protein degradation. Loss of the reductase would significantly lower the activity of the enzyme. The recombinant expression vector will provide a starting point for future ^{13}C-NMR experiments to be conducted on this cytochrome P450.

REFERENCES

1. Montellano, P. R. O. d. *Cytochrome P450 Structure, Mechanism, and Biochemistry* third ed.; Kluwer Academic/Plenum Publishers: New York, 2005.

2. Guengerich, F. P. *J. Biol. Chem.* **1991**, *266*, 10019.

3. Silverman, R. B., *The Organic Chemistry of Drug Design and Drug Action*. Second ed.; Elsevier Academic Press: 2006.

4. Rivera, M., Caignan, G. A., *Anal. Bioanal. Chem.* **2004,** 378, 1464.

5. Alontaga, A. Y., Bunce, R.A., Wilkis, A., Rivera, M. *Inorg. Chem.* **2006**, *45*, 8876.

6. Eakanunkul, S. et al. *Biochemistry* **2005**, 44, 13179.

7. Caignan, G.A.; Deshmukh, R.; Zeng, Y.; Wilks, A.; Bunce, R.A.; Rivera, M., *J. Am. Chem. Soc*. **2003**, 125, 11842.

8. Li, Juncheng; Deslouches, Berthony; Cosloy, Sharon D.; Russell, Charlotte Sananes. *Biochim. Biophys. Acta.* **2003***, 1626, 102.*

9. Rivera, M., Walker, F.A. *Anal. Biochem.* **1995**, *230*, 295.

10. Wang, J., Scott, A.I. *Tetrahedron Lett.* **1997**, *38*, 739.

11. Nakamura, E., Aoki, Kouichi, S., Oshino, S.H., Kuwajima, I. *J. Am. Chem. Soc.* **1987**, *109*, 8056.

12. Chen, Y. P., Woodin, S.A., Lincoln, D.E., Lovell, C.R. *J. Biol. Chem.* **1996**, *271*, 4609.

13. LaCount, M. W., Zhang, E., Chen, Y.P., Han, K., Whitton, M.M., Lincoln, D.E., Woodin, S.A., Lebioda, L. *J. Biol. Chem.* **2000**, *272*, 18712.

14. Osborne, R. L., Taylor, L.O., Han, K.P., Ely, B., Dawson, J.H. *Biochem. Biophys. Res. Commun.* **2004**, *324*, 1194.

15. Niehaus, K., Deng, P., Belyea, J., Franzen, S., Niehause, G.U. *J. Phys. Chem. B.* **2006**, *110*, 13264.

16. Osborne, R. L., Sumithran, S., Coggins, M.K., Chen, Y.P., Lincoln, D.E., Dawson, J.H. *J. Inorg. Biochem.* **2006**, *100*, 1100.

17. Gustafsson, M. C. U., Roitel, O., Marhsall, K.R., Noble, M.A., Chapman, S.K., Pessegueiro, A., Fulco, A.J., Chessma, M.R., Wachenfeldt, C., Munro, A.W. *Biochemistry* **2004**, *43*, 5474.

18. Schwaneberg, U., Schmidt-Dannert, C., Schmitt, J., Schmid, R.D. *Anal. Biochem.* **1999**, *269*, 359.

19. Lussenburg, B. M. A., Babel, Lloyd C., Vermeulen, Nico P.E., Commandeur, Jan N.M. *Anal. Biochem.* **2005**, *341*, 148.

20. Budde, M., Morr, Michael, Schmid, Rolf. D., Urlacher, Vlada B. *Chem. Bio. Chem.* **2006**, *7*, 789.

21. Stratagene pBlueScript II Phagemid Vector. http://www.stratagene.com/products/showProduct.aspx?pid=267

22. Omura, T.; Sato, R. *J. Biol. Chem.* **1964**, 239, 2370.

23. Teale, F.W.J. (1959) *Biochim. Biophys. Acta.* 35, 543.

24. Yonetani, T. (1967), *J. Biol. Chem.* 242, 5008.

25. Kunst, F., Ogasawara, N., Moszer, I., Albertini, A. M., Alloni, G., et al. (1997), *Nature* 390, 249.

26. Budde, M. M., S. C., Schmid, R. D. *Appl. Microbiol. Biotechnol.* **2005**, *66*, 180.

27. Roach, M. P., Chen, Y.P., Woodin, S.A., Lincoln, D.E., Lovell, C.R., Dawson, J.H. *Biochemistry* **1997**, *36*, 2197.

28. Iida, K., Takao, Yuki, Ogai, Tomoe, Kajiwara, Masahiro *J. Label. Compds. Radiopharm.* **1997**, 797.

29. von Weymarn, L. B., Blobaum, A. L., Hollenberg, P.F. *Arch. Biochem. Biophys.* **2004**, *425*, 95.

30. Pflug, S., Richter, Sven M., Urlacher, Vlada B., *J. Biotechnol.* **2007**. doi:10.1016/j.jbiotec.2007.01.013

31. Maurer, S. C., Schulze, Holger, Schmid, Rolf D., Urlacher, Vlad, *Adv. Synth. Catal.* **2003,** 345, 802.